



Systems metabolic engineering of the primary and secondary metabolism of *Streptomyces albidoflavus* enhances production of the reverse antibiotic nybomycin against multi-resistant *Staphylococcus aureus*

Julian Stegmüller^a, Marta Rodríguez Estévez^b, Wei Shu^a, Lars Gläser^a, Maksym Myronovskiy^b, Christian Rückert-Reed^c, Jörn Kalinowski^c, Andriy Luzhetskyy^b, Christoph Wittmann^{a,*}

^a Institute of Systems Biotechnology, Saarland University, Saarbrücken, Germany

^b Department of Pharmaceutical Biotechnology, Saarland University, Saarbrücken, Germany

^c Center for Biotechnology, Bielefeld University, Bielefeld, Germany

ARTICLE INFO

Keywords:

Streptomyces albidoflavus
Streptomyces albus
Staphylococcus aureus
 Antibiotic
 MRSA
 RNA sequencing
 Pentose phosphate pathway
 Shikimic acid pathway
 Export
 Transcriptional regulation
 mCherry
 Reporter strain
 Mannitol
 Fluoroquinolone
 Methicillin
 Gyrase

ABSTRACT

Nybomycin is an antibiotic compound with proven activity against multi-resistant *Staphylococcus aureus*, making it an interesting candidate for combating these globally threatening pathogens. For exploring its potential, sufficient amounts of nybomycin and its derivatives must be synthesized to fully study its effectiveness, safety profile, and clinical applications. As native isolates only accumulate low amounts of the compound, superior producers are needed. The heterologous cell factory *S. albidoflavus* 4N24, previously derived from the cluster-free chassis *S. albidoflavus* Del14, produced 860 $\mu\text{g L}^{-1}$ of nybomycin, mainly in the stationary phase. A first round of strain development modulated expression of genes involved in supply of nybomycin precursors under control of the common P_{erm^*} promoter in 4N24, but without any effect. Subsequent studies with mCherry reporter strains revealed that P_{erm^*} failed to drive expression during the product synthesis phase but that use of two synthetic promoters (P_{kasOP^*} and P_{41}) enabled strong constitutive expression during the entire process. Using P_{kasOP^*} , several rounds of metabolic engineering successively streamlined expression of genes involved in the pentose phosphate pathway, the shikimic acid pathway, supply of CoA esters, and nybomycin biosynthesis and export, which more than doubled the nybomycin titer to 1.7 mg L^{-1} in the sixth-generation strain NYB-6B. In addition, we identified the minimal set of *nyb* genes needed to synthesize the molecule using single-gene-deletion strains. Subsequently, deletion of the regulator *nybW* enabled nybomycin production to begin during the growth phase, further boosting the titer and productivity. Based on RNA sequencing along the created strain genealogy, we discovered that the *nyb* gene cluster was unfavorably downregulated in all advanced producers. This inspired removal of a part and the entire set of the four regulatory genes at the 3'-end *nyb* of the cluster. The corresponding mutants NYB-8 and NYB-9 exhibited marked further improvement in production, and the deregulated cluster was combined with all beneficial targets from primary metabolism. The best strain, *S. albidoflavus* NYB-11, accumulated up to 12 mg L^{-1} nybomycin, fifteenfold more than the basic strain. The absence of native gene clusters in the host and use of a lean minimal medium contributed to a selective production process, providing an important next step toward further development of nybomycin.

1. Introduction

Fluoroquinolones are among the most frequently prescribed antibiotics. These compounds target bacterial DNA gyrase, which is involved in DNA replication, by binding the enzyme-DNA complex and blocking subsequent ligation of double-strand breaks (Aldred et al., 2014; Drlica et al., 2009). Typically, the mode of action involves binding of the

antibiotic to a serine residue of the *gyrA* subunit of the protein via a hydrated magnesium ion bridge (Blower et al., 2016). However, the prevalence of and increase in fluoroquinolone resistance (FQR) are significant concerns (Parkinson et al., 2015b). Prominent pathogens acquire FQR through mutation of the *gyrA* gene that replaces a serine residue, including FQR methicillin-resistant *Staphylococcus aureus* (S84L) (Hiramatsu et al., 2012), *Bacillus anthracis* (S85L) (Price et al.,

* Corresponding author.

E-mail address: christoph.wittmann@uni-saarland.de (C. Wittmann).

<https://doi.org/10.1016/j.ymben.2023.12.004>

Received 11 August 2023; Received in revised form 17 November 2023; Accepted 1 December 2023

Available online 9 December 2023

1096-7176/© 2023 The Authors. Published by Elsevier Inc. on behalf of International Metabolic Engineering Society. This is an open access article under the CC BY license (<http://creativecommons.org/licenses/by/4.0/>).

2003), *E. coli* (S83L) (Vila et al., 1994), *Acinetobacter baumannii* (S83L) (Vila et al., 1995), vancomycin-resistant *Enterococcus* (S83I/R/Y) (Werner et al., 2010), and *Klebsiella pneumoniae* (S8F/Y) (Deguchi et al., 1997). Remarkably, compounds from the nybomycin (nybomycin, deoxynybomycins, and derivatives) class of natural products display potent efficacy against FQR methicillin-resistant *S. aureus* and vancomycin-resistant enterococci in mouse models, and they effectively inhibit mutated DNA gyrase (S84L) *in vitro* (Parkinson et al., 2015b). It has been reported that a majority of FQR methicillin-resistant *S. aureus* was eliminated in mice when they were exposed to nybomycins. Sequence analysis of the few survivors revealed a backmutation in the *gyrA* gene that rendered the mutants susceptible to fluoroquinolones again. This feature led to the creation of the term ‘reverse antibiotic’ (Hiramatsu et al., 2012, 2015; Parkinson et al., 2015a). In addition to nybomycin, apigenin, a compound from the flavone class, shows such ‘reverse antibiotic’ activity against FQR methicillin-resistant *S. aureus* (Morimoto et al., 2015). It has been concluded that concurrent application of nybomycins and fluoroquinolones might counteract resistance in these pathogens and restore fluoroquinolone efficacy to fight against them (Bardell-Cox et al., 2019). Additionally, nybomycins exhibit antibiotic effectiveness against dormant *Mycobacterium tuberculosis*, along with a variety of other gram-positive and gram-negative bacteria (Arai et al., 2015; Strelitz et al., 1955). Further studies revealed activity against different cancer cell lines, including A549 (human lung), VA13 (lung fibroblast) (Zakalyukina et al., 2019), Saos-2 (human osteoblastic sarcoma), TMK-1 (gastric cancer) and THP-1 (monocytic leukemia), though survival of normal human fibroblasts was not affected (Egawa et al., 2000). The remaining challenges of nybomycins include low aqueous solubility and selectivity issues regarding human topoisomerase isoforms (Hergenrother and Leys, 2018). Notably, medicinal chemistry has provided nybomycin derivatives with increased bioavailability and novel activity against relevant gram-negative pathogens (Richter et al., 2017). Further drug optimization studies may overcome these issues and advance this class of antibiotics into clinical trials (Bardell-Cox et al., 2019). Such important research, in turn, requires a sufficient supply of compounds.

In this regard, researchers recently discovered natural producers of nybomycins, including *Streptomyces* sp. AD-3-6 (Wang et al., 2019), *Streptomyces hyalinus* (Komaki et al., 2020), and *S. albus* subsp. *chlorinus* NRRL B-24108 (Rodríguez Estevez et al., 2018). *Streptomyces* sp. AD-3-6 was found to produce nybomycin at a concentration of 2.5 mg L⁻¹ (Wang et al., 2019); *S. albus* subsp. *chlorinus* NRRL B-24108, currently the most productive natural isolate, yielded a concentration of 15 mg L⁻¹ (Kuhl et al., 2021). However, strain NRRL B-24108 showed genetic inaccessibility in subsequent studies (Myronovskiy et al., 2020), hindering its optimization through metabolic engineering. Despite these discoveries, fermentative production of nybomycin remains inefficient, with reports indicating that 1000 L of fermentation yields only 200–350 mg of nybomycin (Bardell-Cox et al., 2019). Conversely, while total synthesis of nybomycin has been achieved, it is hampered by low overall yields, recorded at 0.84% (Bardell-Cox et al., 2019; Forbis and Rinehart, 1970, 1971, 1973), 11% (Parkinson et al., 2015b), and 13% (Nussbaum et al., 2009).

Considering the constraints of both chemical synthesis and biosynthesis in natural sources, development of nybomycin through heterologous production in engineered recombinant hosts is a promising approach at this stage. In this regard, recent successful transfer and expression of the 35 kb *nyb* biosynthesis-related gene cluster from *S. albus* subsp. *chlorinus* NRRL B-24108 (Fig. 1A) into the well-established production host *S. albidoflavus* Del14 (formerly known as *S. albus* Del14) marks a significant advancement (Rodríguez Estevez et al., 2018). This development led to creation of the derivative *S. albidoflavus* 4N24, facilitating the first instance of heterologous nybomycin production (Rodríguez Estevez et al., 2018). The deciphered biosynthetic pathway, as inferred from the predicted functions of *nyb* genes, presents a multifaceted process. Synthesis of the antibiotic

involves integration of precursors from multiple metabolic pathways, including the Emden-Meyerhof-Parnas (EMP), pentose phosphate (PP), ethyl-malonyl-CoA, and shikimic acid (SA) pathways. These converge in a complex, nine-step assembly line, culminating in formation of the active nybomycin molecule (Fig. 1B). Research indicates that an abundant supply of product precursors is a critical aspect of highly productive cell factories (Kind et al., 2014; Pauli et al., 2023; Rohles et al., 2018, 2022; Weiland et al., 2023), suggesting that enhancing related pathways in primary metabolism may be a key strategy for boosting nybomycin production. Hence, nybomycin is an interesting model case from the metabolic engineering viewpoint, given the various supporting pathways involved.

In this study, our objective was to metabolically engineer *S. albidoflavus* 4N24 to augment nybomycin production. Initially, we thoroughly analyzed the *nyb* gene cluster and, via a series of targeted gene deletions, pinpointed essential genes for biosynthesis of the compound. After identifying the most effective promoters for high-level, dynamic gene expression in the host, we embarked on multiple rounds of metabolic engineering. This process involved strategic modifications to key genes within the pentose phosphate (PP) pathway, shikimic acid (SA) pathway, CoA ester supply, and pathways for nybomycin biosynthesis and export. These alterations successively enhanced the production yield from 0.9 mg L⁻¹ in the original 4N24 strain to 1.8 mg L⁻¹ in the sixth-generation variant *S. albidoflavus* NYB-6B. Furthermore, comparative transcriptomic analyses across different producing strains revealed an unexpected reduction in *nyb* cluster expression during peak production. This insight led to development of the synthetic mutants NYB-8 and NYB-9, which harbored partial or complete deletions of the *nyb* regulatory genes, namely, $\Delta nybWX$ and $\Delta nybWXYZ$, respectively, resulting in extended synthesis periods. The culmination of these efforts was generation of the advanced genome-engineered strains *S. albidoflavus* NYB-10 and NYB-11, which integrate all favorable modifications to both primary and secondary metabolism, ultimately achieving a nybomycin titer of 12 mg L⁻¹.

2. Materials and methods

2.1. Strains

S. albidoflavus Del14, formerly known as *S. albus* Del14, and its derivative 4N24 were obtained from previous work (Rodríguez Estevez et al., 2018). *Streptomyces* sp. GBA 94–10 (Ian et al., 2014) served as donor of genomic DNA. *E. coli* DH10B was used for general cloning purposes (Thermo Fisher Scientific, Karlsruhe, Germany). *E. coli* ET12567/pUZ8002 served as a donor for intergenic conjugation (Kieser et al., 2000). All strains and plasmids used in this study are listed in Table 1.

2.2. Media

E. coli strains were cultured in liquid Lucia-Bertani (LB) medium. Solid LB medium was obtained by adding 20 g L⁻¹ agar (Becton Dickinson, Heidelberg, Germany). For sporulation, *S. albidoflavus* was grown on MS agar containing 20 g of D-mannitol (Sigma Aldrich, Taufkirchen, Germany), 20 g of soy flour (Schoenenberger Hensel, Magstadt, Germany), and 20 g of agar (Becton Dickinson) per liter. When needed, kanamycin (50 µg mL⁻¹), hygromycin B (50 µg mL⁻¹ for *Streptomyces*, 100 µg mL⁻¹ for *E. coli*), and apramycin (50 µg mL⁻¹) were added for selection. When using suicide vectors for in-frame deletion of genes of interest, 5-bromo-4-chloro-1H-indol-3-yl β-D-glucopyranosiduronic acid (X-Gluc, 40 µg mL⁻¹) was added to the LB plate medium for blue-white screening. For nybomycin production, strains were precultured in liquid ISP medium (pH 7.2) containing 3 g of yeast extract (Beckton Dickinson) and 5 g of tryptone (Beckton Dickinson) per liter. For secondary metabolite expression and *nyb* cluster characterization, *S. albidoflavus* strains were grown in liquid DNPM medium (40 g L⁻¹

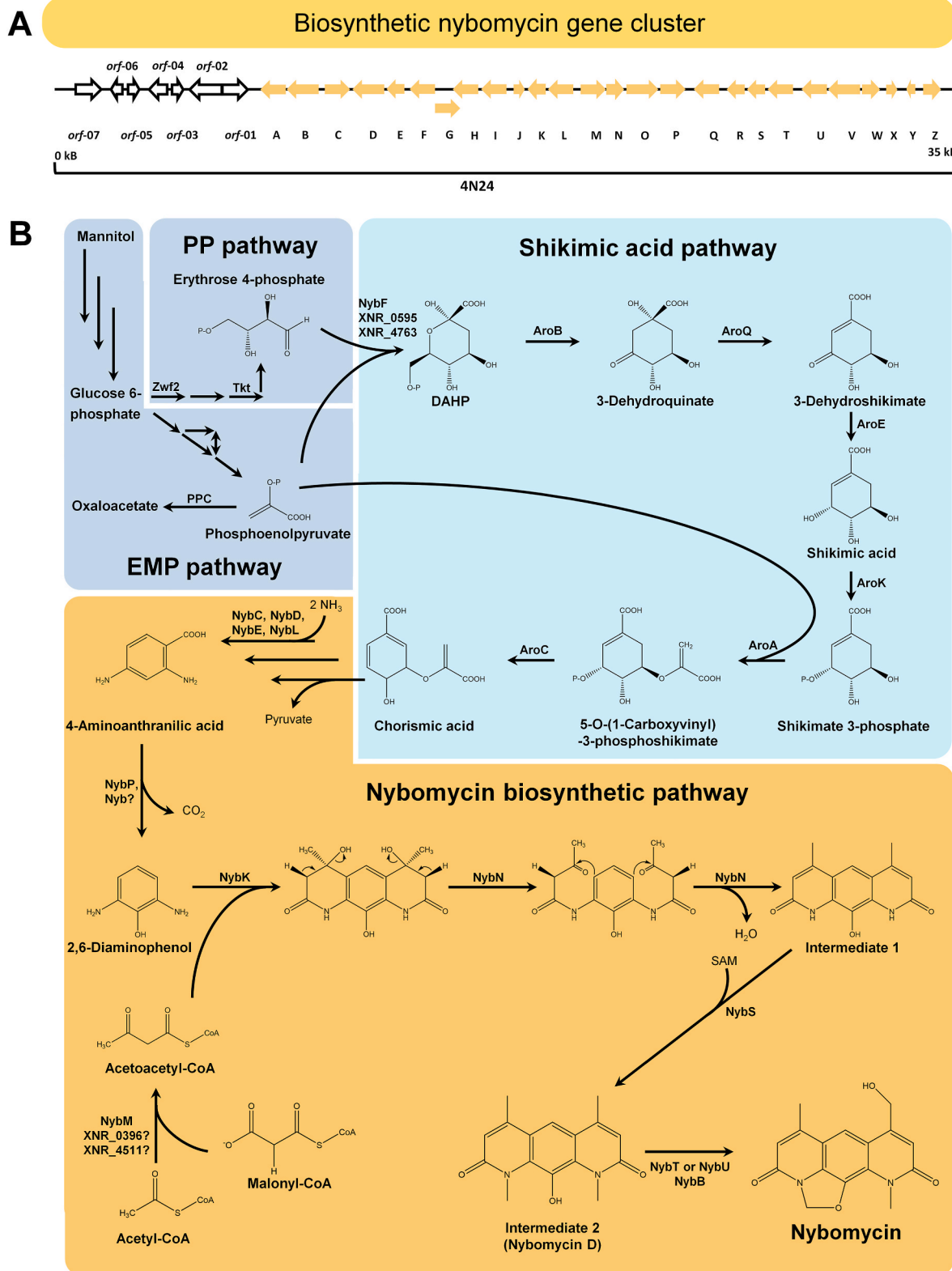


Fig. 1. Genetics and biochemistry of nybomycin biosynthesis in *Streptomyces*. The data show the *nyb* encoding gene cluster from *S. albus* subsp. *chlorinus* NRRL B-24108 (Rodriguez Estevez et al., 2018) (A) and the suggested biosynthetic pathway (B). For the latter, erythrose 4-phosphate (E4P) and phosphoenolpyruvate (PEP) are supplied from the PP and EMP pathways to yield shikimic acid and chorismic acid, mainly via endogenous aromatic amino acid biosynthesis (AroABCEKQ) (Euverink, 1995; Parthasarathy et al., 2018). Further conversion into 2,6-diaminophenol via 4-aminoanthranilic acid is encoded by the genes *nybC*, *nybD*, *nybE*, *nybL* and *nybP*. Next, the aromatic ring is extended by the attachment of two acetoacetyl-CoA residues, followed by closure of the pyridine rings and methylation of the two nitrogen atoms. The subsequent formation of an oxazoline ring provides deoxy-nybomycin, which is ultimately hydroxylated to yield nybomycin (Rodriguez Estevez et al., 2018).

Table 1
Strains and plasmids.

Strains/Plasmids	Description	Reference
Strains		
<i>E. coli</i>		
DH10B	F– mcrA Δ(mrr-hsdRMS-mcrBC) φ80lacZΔM15 ΔlacX74 recA1 endA1 araD139 Δ (ara-leu)7697 galU galK λ– rpsL (Str ^R) nupG	Thermo Fisher Scientific
ET12567/pUZ8002	Nonmethylating ET12567 containing nontransmissible RP4 derivative plasmid pUZ8002, Cm ^R , Kan ^R	Kieser et al. (2000)
<i>Streptomyces</i> sp.		
GBA 94–10	Donor of genomic DNA for cloning purposes	Ian et al. (2014)
<i>S. albidoflavus</i>		
4N24	<i>S. albidoflavus</i> Del14, formerly <i>S. albus</i> Del14, expressing BAC 4N24 for heterologous nybomycin production	Rodriguez Estevez et al. (2018)
4N24 Δorf-07	4N24 with in-frame deletion of <i>orf-07</i>	This work
4N24 Δorf-06	4N24 with in-frame deletion of <i>orf-06</i>	This work
4N24 Δorf-05	4N24 with in-frame deletion of <i>orf-05</i>	This work
4N24 Δorf-04	4N24 with in-frame deletion of <i>orf-04</i>	This work
4N24 Δorf-03	4N24 with in-frame deletion of <i>orf-03</i>	This work
4N24 Δorf-02	4N24 with in-frame deletion of <i>orf-02</i>	This work
4N24 Δorf-01	4N24 with in-frame deletion of <i>orf-01</i>	This work
4N24 ΔnybA	4N24 with in-frame deletion of <i>nybA</i>	This work
4N24 ΔnybB	4N24 with in-frame deletion of <i>nybB</i>	This work
4N24 ΔnybC	4N24 with in-frame deletion of <i>nybC</i>	This work
4N24 ΔnybT	4N24 with in-frame deletion of <i>nybT</i>	This work
4N24 ΔnybU	4N24 with in-frame deletion of <i>nybU</i>	This work
4N24 ΔnybV	4N24 with in-frame deletion of <i>nybV</i>	This work
4N24 ΔnybX	4N24 with in-frame deletion of <i>nybX</i>	This work
4N24 ΔnybY	4N24 with in-frame deletion of <i>nybY</i>	This work
4N24 ΔnybZ	4N24 with in-frame deletion of <i>nybZ</i>	This work
NYB-1A	4N24 expressing <i>tkf</i> (B591_RS24355) from <i>Streptomyces</i> sp. GBA 94–10 under control of <i>P_{ermE}</i> *	This work
NYB-1B	4N24 expressing <i>zwf2</i> (B591_RS24345) from <i>Streptomyces</i> sp. GBA 94–10 under control of <i>P_{ermE}</i> *	This work
NYB-1C	4N24 expressing <i>arol</i> (NCgl0950) with the amino acid exchange S187C from <i>C. glutamicum</i> ATCC 13032 under control of <i>P_{ermE}</i> *	This work
NYB-2A	4N24 expressing <i>tkf</i> (B591_RS24355) from <i>Streptomyces</i> sp. GBA 94–10 under control of <i>P_{kasOP}</i> *	This work
NYB-2B	4N24 expressing <i>zwf2</i> (B591_RS24345) from <i>Streptomyces</i> sp. GBA 94–10 under control of <i>P_{kasOP}</i> *	This work
NYB-2C	4N24 with in-frame deletion of <i>ppc</i> (XNR, 2069)	This work
NYB-2D	4N24 expressing <i>arog</i> (P0AB91) with the amino acid exchange D146N from <i>E. coli</i> K12 under control of <i>P_{kasOP}</i> *	This work
NYB-2E	4N24 expressing <i>arol</i> (NCgl0950) with the amino acid exchange S187C from <i>C. glutamicum</i> ATCC 13032 under control of <i>P_{kasOP}</i> *	This work
NYB-2F	4N24 expressing <i>nybF</i> (FM076_RS29120) from <i>S. albus</i> subsp. <i>chlorinus</i> NRRL B-24108 under control of <i>P_{kasOP}</i> *	This work
NYB-3A	4N24 expressing <i>nybM</i> (FM076_RS29150) from <i>S. albus</i> subsp. <i>chlorinus</i> NRRL B-24108 under control of <i>P_{kasOP}</i> *	This work
NYB-3B	4N24 expressing <i>nybV</i> (FM076_RS2919) from <i>S. albus</i> subsp. <i>chlorinus</i> NRRL B-24108 under control of <i>P_{kasOP}</i> *	This work
NYB-4A	4N24 expressing <i>tkf</i> (B591_RS24355) and <i>zwf2</i> (B591_RS24345) from <i>Streptomyces</i> sp. GBA 94–10 under control of <i>P_{kasOP}</i> *	This work
NYB-4B	4N24 expressing <i>nybF</i> (FM076_RS29120) from <i>S. albus</i> subsp. <i>chlorinus</i> NRRL B-	This work

Table 1 (continued)

Strains/Plasmids	Description	Reference
	24108 and <i>zwf2</i> (B591_RS24345) from <i>S. albidoflavus</i> sp. GBA 94–10 under control of <i>P_{kasOP}</i> *	
NYB-4C	4N24 expressing <i>nybF</i> (FM076_RS29120) from <i>S. albus</i> subsp. <i>chlorinus</i> NRRL B-24108 and <i>tkf</i> (B591_RS24355) from <i>Streptomyces</i> sp. GBA 94–10 under control of <i>P_{kasOP}</i> *	This work
NYB-4D	4N24 expressing <i>nybF</i> (FM076_RS29120) from <i>S. albus</i> subsp. <i>chlorinus</i> NRRL B-24108, <i>tkf</i> (B591_RS24355), and <i>zwf2</i> (B591_RS24345) from <i>Streptomyces</i> sp. GBA 94–10 under control of <i>P_{kasOP}</i> *	This work
NYB-5	4N24 with in-frame deletion of <i>nybW</i>	This work
NYB-6A	NYB-5 expressing <i>tkf</i> (B591_RS24355) and <i>zwf2</i> (B591_RS24345) from <i>Streptomyces</i> sp. GBA 94–10 under control of <i>P_{kasOP}</i> *	This work
NYB-6B	NYB-5 expressing <i>nybF</i> (FM076_RS29120) from <i>S. albus</i> subsp. <i>chlorinus</i> NRRL B-24108 and <i>zwf2</i> (B591_RS24345) from <i>Streptomyces</i> sp. GBA 94–10 under control of <i>P_{kasOP}</i> *	This work
NYB-6C	NYB-5 expressing <i>nybF</i> (FM076_RS29120) from <i>S. albus</i> subsp. <i>chlorinus</i> NRRL B-24108 and <i>tkf</i> (B591_RS24355) from <i>Streptomyces</i> sp. GBA 94–10 under control of <i>P_{kasOP}</i> *	This work
NYB-7	NYB-5 expressing <i>nybF</i> (FM076_RS29120) from <i>S. albus</i> subsp. <i>chlorinus</i> NRRL B-24108, and <i>tkf</i> (B591_RS24355) and <i>zwf2</i> (B591_RS24345) from <i>Streptomyces</i> sp. GBA 94–10 under control of <i>P_{kasOP}</i> *	This work
NYB-8	4N24 with in-frame deletion of <i>nybWX</i>	This work
NYB-9	4N24 with in-frame deletion of <i>nybWXYZ</i>	This work
NYB-10	NYB-8 expressing <i>nybF</i> (FM076_RS29120) from <i>S. albus</i> subsp. <i>chlorinus</i> NRRL B-24108 and <i>zwf2</i> (B591_RS24345) from <i>Streptomyces</i> sp. GBA 94–10 under control of <i>P_{kasOP}</i> *	This work
NYB-11	NYB-9 expressing <i>nybF</i> (FM076_RS29120) from <i>S. albus</i> subsp. <i>chlorinus</i> NRRL B-24108 and <i>zwf2</i> (B591_RS24345) from <i>Streptomyces</i> sp. GBA 94–10 under control of <i>P_{kasOP}</i> *	This work
RFP-1	4N24 expressing <i>mCherry</i> under control of <i>P_{ermE}</i> *	This work
RFP-2	4N24 expressing <i>mCherry</i> under control of <i>P_{tipA}</i>	This work
RFP-3	4N24 expressing <i>mCherry</i> under control of <i>P_{SF14}</i>	This work
RFP-4	4N24 expressing <i>mCherry</i> under control of <i>P₂₁</i>	This work
RFP-5	4N24 expressing <i>mCherry</i> under control of <i>P_{SP43}</i>	This work
RFP-6	4N24 expressing <i>mCherry</i> under control of <i>P_{SP44}</i>	This work
RFP-7	4N24 expressing <i>mCherry</i> under control of <i>P_{kasOP}</i> *	This work
RFP-8	4N24 expressing <i>mCherry</i> under control of <i>P_{SP41}</i>	This work
Plasmids/BACs		
4N24	BAC containing the nybomycin biosynthetic gene cluster	Rodriguez Estevez et al. (2018)
4N24 ΔnybW	4N24 with in-frame replacement of <i>nybW</i> (FM076_RS29200) by Kan ^R	This work
4N24 ΔnybWX	4N24 with in-frame replacement of <i>nybW</i> (FM076_RS29200), <i>nybX</i> (FM076_RS29205) by Kan ^R	This work
4N24 ΔnybWXYZ	4N24 with in-frame replacement of <i>nybW</i> (FM076_RS29200), <i>nybX</i> (FM076_RS29205), <i>nybY</i> (FM076_RS29210), and <i>nybZ</i> (FM076_RS29215) by Kan ^R	This work

(continued on next page)

Table 1 (continued)

Strains/Plasmids	Description	Reference
pRT801	Integrative plasmid containing <i>oriT</i> , <i>attP</i> , <i>int</i> <i>phiBT1</i> , and <i>aac3(IV)</i>	Gregory et al. (2003)
pKG1132	Suicide vector for genome-based modification of actinobacteria, comprising <i>ori</i> for <i>E. coli</i> , and <i>Am^R</i> and <i>gusA</i> as selection markers	Barton et al. (2018)
pKG1132hyg	Suicide vector for genome-based modification of actinobacteria, comprising <i>ori</i> for <i>E. coli</i> , and <i>Am^R</i> and <i>gusA</i> as selection markers	Gläser et al. (2021b)
pDppc4	Suicide vector derivative of pKG1132hyg for in-frame deletion of XNR 2069 in 4N24	This work
pBT1H	Integrative plasmid containing <i>oriT</i> , <i>attP</i> , <i>int</i> <i>phiBT1</i> , <i>hph</i> ,	This work
pBT1HP	Integrative plasmid containing <i>oriT</i> , <i>attP</i> , <i>int</i> <i>phiBT1</i> , <i>hph</i> , <i>P_{ermE*}</i> , <i>tfd</i>	This work
pBT1H <i>tkl1</i>	integrative plasmid containing <i>P_{ermE*}</i> <i>tkl1</i> , <i>Hyg^R</i>	This work
pBT1H <i>zwf2</i>	integrative plasmid containing <i>P_{ermE*}</i> <i>zwf2</i> , <i>Hyg^R</i>	This work
pBT1HP <i>arofibr</i>	integrative plasmid containing <i>P_{ermE*}</i> <i>arofibr</i> , <i>Hyg^R</i>	This work
pBT1HP <i>ermCherry</i>	integrative plasmid containing <i>P_{ermE*}</i> <i>mCherry</i> , <i>Hyg^R</i>	This work
pBT1H-kasOP* <i>mCherry</i>	integrative plasmid containing <i>P_{kasOP*}</i> <i>mCherry</i> , <i>Hyg^R</i>	This work
pBT1H-P21 <i>mCherry</i>	integrative plasmid containing <i>P₂₁</i> <i>mCherry</i> , <i>Hyg^R</i>	This work
pBT1H-PtipA <i>mCherry</i>	integrative plasmid containing <i>P_{tipA}</i> <i>mCherry</i> , <i>Hyg^R</i>	This work
pBT1H-SF14P <i>mCherry</i>	integrative plasmid containing <i>P_{SF14}</i> <i>mCherry</i> , <i>Hyg^R</i>	This work
pBT1H-SP41 <i>mCherry</i>	integrative plasmid containing <i>P_{SP41}</i> <i>mCherry</i> , <i>Hyg^R</i>	This work
pBT1H-SP43 <i>mCherry</i>	integrative plasmid containing <i>P_{SP43}</i> <i>mCherry</i> , <i>Hyg^R</i>	This work
pBT1H-SP44 <i>mCherry</i>	integrative plasmid containing <i>P_{SP44}</i> <i>mCherry</i> , <i>Hyg^R</i>	This work
pBT1H-kasOP* <i>tkl1</i>	integrative plasmid containing <i>P_{kasOP*}</i> <i>tkl1</i> , <i>Hyg^R</i>	This work
pBT1H-kasOP* <i>zwf2</i>	integrative plasmid containing <i>P_{kasOP*}</i> <i>zwf2</i> , <i>Hyg^R</i>	This work
pBT1H-kasOP* <i>nybV</i>	integrative plasmid containing <i>P_{kasOP*}</i> <i>nybV</i> , <i>Hyg^R</i>	This work
pBT1H-kasOP* <i>nybM</i>	integrative plasmid containing <i>P_{kasOP*}</i> <i>nybM</i> , <i>Hyg^R</i>	This work
pBT1H- <i>pkasOP*</i> <i>nybF</i>	integrative plasmid containing <i>P_{kasOP*}</i> <i>nybF</i> , <i>Hyg^R</i>	This work
pBT1H- <i>kasOP*</i> <i>aroGfbr</i>	integrative plasmid containing <i>P_{kasOP*}</i> <i>aroGfbr</i> , <i>Hyg^R</i>	This work
pBT1H- <i>kasOP*</i> <i>arofibr</i>	integrative plasmid containing <i>P_{kasOP*}</i> <i>arofibr</i> , <i>Hyg^R</i>	This work
pBT1H- <i>kasOP*</i> <i>nybF</i> <i>zwf2</i>	integrative plasmid containing <i>P_{kasOP*}</i> <i>nybF</i> , <i>zwf2</i> , <i>Hyg^R</i>	This work
pBT1H- <i>kasOP*</i> <i>nybF</i> <i>tkl1</i>	integrative plasmid containing <i>P_{kasOP*}</i> <i>nybF</i> , <i>tkl1</i> , <i>Hyg^R</i>	This work
pBT1H- <i>kasOP*</i> <i>tkl1</i> <i>zwf2</i>	integrative plasmid containing <i>P_{kasOP*}</i> <i>tkl1</i> , <i>zwf2</i> , <i>Hyg^R</i>	This work
pBT1H <i>kasOP*</i> <i>nybF</i> <i>tkl1</i> <i>zwf2</i>	integrative plasmid containing <i>P_{kasOP*}</i> <i>nybF</i> , <i>tkl1</i> , <i>zwf2</i> , <i>Hyg^R</i>	This work

dextrin, 7.5 g L⁻¹ soytone, 5 g L⁻¹ yeast extract, and 21 g L⁻¹ MOPS, pH 6.8). The main cultures for production of nybomycin were grown in chemically defined medium containing the following per liter: 10 g of D-mannitol, 15 g of (NH₄)₂SO₄, 20.9 g of MOPS, 0.5 g of K₂HPO₄, 1 g of NaCl, 0.55 g of CaCl₂, 0.2 g of MgSO₄·7H₂O, 0.02 g of FeSO₄·7H₂O, 2 mg of FeCl₃·6H₂O, 2 mg of MnSO₄·H₂O, 0.5 mg of ZnSO₄·H₂O, 0.5 mg of CuCl₂·2H₂O, 0.2 mg of Na₂B₄O₇·10H₂O, 0.1 mg of (NH₄)₆Mo₇O₂₄·4H₂O, 1 mg of nicotinamide, 1 mg of riboflavin, 0.5 mg of thiamine hydrochloride, 0.5 mg of pyridoxine hydrochloride, 0.2 mg of biotin, and 0.1 mg of *p*-aminobenzoic acid.

2.3. Molecular biology and genetic engineering

SnapGene software (GSL Biotech LLC, San Diego, CA, USA) was used for strain, plasmid, and primer design. Selected gene deletions were introduced into BAC 4N24 in *E. coli* using RedET cloning (Myronovskiy et al., 2018). DNA fragments of interest were amplified by PCR (2 × Phusion High-Fidelity PCR Master Mix with GC Buffer, Thermo Scientific, Waltham, MA, USA) using sequence-specific primers (Supplementary File 1, Table S1). Prior to assembly, the amplified fragments were extended with 20 bp overhangs at their 5'-end. Afterward, they were purified (Wizard SV Gel, PCR Clean-Up System, Promega, Mannheim, Germany) and assembled *in vitro* with the linearized vector. The latter was obtained by treatment with endonucleases (*EcoRV*, *SnaBI*, *PvuII*) and alkaline phosphatase. The reaction mixture contained 157.5 mM Tris-HCl (pH 7.5), 15.75 mM MgCl₂, 15.75 mM DTT, 42 mg μL⁻¹ PEG-800, 0.6 mg μL⁻¹ NAD, 25 mU μL⁻¹ Phusion High-Fidelity DNA Polymerase (Thermo Fisher Scientific), 7.5 mU μL⁻¹ T5 exonuclease (Epicentre, Madison, WI, USA), 4 U μL⁻¹ Taq Ligase (Thermo Fisher Scientific), and 0.3 mM dNTPs. The assembled plasmids were transferred into *E. coli* DH10B cells by heat shock (Sambrook and Russell, 2001), followed by selection. Subsequently, the plasmids were multiplied in the cloning host, isolated (QIAprep Spin MiniPrep Kit, Qiagen, Hilden, Germany), verified for correctness by PCR, subjected to restriction digestion and sequencing (Genewiz Germany GmbH, Leipzig, Germany), transferred into the methylation-deficient donor *E. coli* ET12567/pUZ8002 for amplification, and subsequently transferred into *S. albidoflavus* by intergenic conjugation (Kieser et al., 2000). In short, spores obtained from four-day-old mannitol soy (MS) agar plates were washed off using sterile water, mixed with *E. coli* ET12567/pUZ8002 (containing the recombinant plasmid of interest) and plated on fresh MS agar. After incubation for 16 h at 30 °C, the plates were overlaid with phosphomycin (200 μg mL⁻¹) and hygromycin (50 μg mL⁻¹). Exconjugants were passaged on fresh MS plates containing phosphomycin and hygromycin. The desired genomic integration was verified by PCR and sequencing. Integrase-mediated site-specific recombination involving *phiBT1* integrase and its associated *attP* attachment site was used to integrate expression plasmids into the genomic locus XNR_3921 (integral membrane protein) of *S. albidoflavus* (Gregory et al., 2003). When using suicide plasmids for in-frame gene deletion, 3 μL X-Gluc (100 mg mL⁻¹) was sprinkled onto spores. After 20–30 min of incubation at 30 °C, the spores were evaluated for blue coloration. Blue-stained exconjugants that had undergone a single crossover were passaged on MS agar without selection pressure, washed off, diluted serially, and plated on MS agar supplemented with X-Gluc (40 μg mL⁻¹) to screen for white colonies that had undergone the second crossover. White colonies were analyzed by PCR to differentiate between the desired mutant and reverted wildtype. For gene deletion within the nybomycin cluster, the gene to be removed was individually replaced via Red/ET recombining by a resistance marker that was later removed. The resulting knockout BAC variants were introduced into *S. albidoflavus* Del14 via conjugation.

2.4. Cultivation in shake flasks for nybomycin production

Liquid cultures were incubated in 500 mL baffled shake flasks filled with 50 mL of medium and 30 g of glass beads (soda-lime glass, 5 mm, Sigma-Aldrich) on an orbital shaker (230 rpm, 75% relative humidity, 28 °C, 5 cm shaking diameter, Multitron, Infors AG, Bottmingen, Switzerland). Spores from a single colony of a plate culture were harvested and inoculated into the first preculture on ISP medium, which was incubated overnight. Then, the cells were collected (5000×g, 25 °C, 6 min) and resuspended in minimal or complex medium for a second preculture, followed by incubation overnight. Afterward, the cells were collected (5000×g, 25 °C, 6 min) and used to inoculate the main culture in minimal or complex medium, as described below. All growth and production experiments were conducted in biological triplicates.

2.5. Cultivation at the miniaturized scale for promoter screening

The first and second precultures were performed in shake flasks, as described above. The screening experiments were conducted in a microplate-based microbioreactor (Biolector I, Beckman Coulter GmbH, Baesweiler, Germany) using 48-well flower plates filled with 1 mL of minimal mannitol medium each and incubated at 1300 rpm, 28 °C, and 80% relative humidity (Becker et al., 2018; Christmann et al., 2023). The cultures were monitored online using photometric measurement of the optical density at 620 nm (OD_{620}) and fluorescence-based quantification of expression of mCherry (Kohlstedt et al., 2018). All experiments were conducted in triplicate.

2.6. Quantification of cell concentration

Cells from cultures on minimal medium with 10 g L⁻¹ mannitol were collected by centrifugation (5000×g, 4 °C, 6 min) and washed twice with 0.9% NaCl. Subsequently, the pellets were freeze-dried, and the cell dry weight (CDW) was gravimetrically measured (HB43-S, Mettler-Toledo, Columbus, OH, USA) (Kuhl et al., 2020). In addition, the cell concentration was analyzed by measuring the optical density (OD_{600}) at 600 nm. Measurements were conducted in triplicate. Systematic analysis of *S. albidoflavus* 4N24 cultures yielded a linear correlation between CDW and OD_{600} , which was valid for the entire cultivation: $CDW [g L^{-1}] = 0.438 \times OD_{600}$ (Supplementary file 1, Fig. S1). The correlation revealed that OD_{600} readings for the shake flask cultures provided a rough estimate of CDW (Kuhl et al., 2020).

2.7. Quantification of sugars and inorganic ions

Mannitol was quantified by isocratic HPLC (Agilent Series 1260 Infinity, Agilent) using an Aminex HPX-87H column (300 × 7.8 mm 9 μm, Bio-Rad, Hercules, CA, USA) at 65 °C as the stationary phase and 3 mM H₂SO₄ as the mobile phase at a flow rate of 0.5 mL min⁻¹ (Hoffmann et al., 2018). Detection and quantification were accomplished by refractive index measurement using external standards. Phosphate was quantified by HPIC (Dionex Integrion, Thermo Fisher Scientific), as previously described (Kuhl et al., 2020). Ammonium was analyzed by HPIC (Dionex Integrion, Thermo Fisher Scientific) using a Dionex IonPac CS16-4 μm column (2 × 250 mm, Thermo Fisher Scientific), 30 mM methanesulfonic acid as the mobile phase (40 °C, 0.16 mL min⁻¹) (Jovanovic Gasovic et al., 2023), and conductivity measurement. External standards were used for quantification.

2.8. Secondary metabolite extraction and characterization

Metabolites were extracted from the culture supernatant using n-butanol, evaporated, and dissolved in methanol. A sample of 1 μL was then separated using a Dionex Ultimate 3000 UPLC (Thermo Fisher Scientific), a reversed-phase column (ACQUITY UPLC BEH C18 column, 100 mm, 1.7 μm, Waters, Milford, MA, USA), and a linear gradient of 0.1% formic acid in acetonitrile against 0.1% formic acid in water (5%–95% in 18 min) at a flow rate of 0.6 mL min⁻¹. The analytes were detected and characterized for fragmentation patterns and accurate masses using an amaZon speed MS ion trap (Bruker, Billerica, MA, USA) and a maXis high-resolution LC-QTOF, respectively (Bruker). Data were collected and analyzed using Bruker Compass Data Analysis software (version 4.1, Bruker).

2.9. Quantification of nybomycin

Nybomycin was extracted from culture broth using n-butanol. In short, 200 μL of broth was mixed with 600 μL of n-butanol and incubated for 15 min (1400 rpm, 23 °C, Thermomixer F1.5 Eppendorf, Wesseling, Germany). The organic phase was collected (20,000×g, 5 min, 4 °C), and 400 μL of n-butanol was mixed with the aqueous phase for a second

extraction step. Afterward, the two organic fractions were collected, and the solvent was removed by freeze drying. The obtained solid was dissolved in a mixture of methanol and DMSO (1:1) and clarified from debris (20,000×g, 10 min, 4 °C). Quantification of nybomycin was conducted by LC-ESI-MS/MS using an HPLC system (Agilent Infinity, 1290 System, Santa Clara, CA, USA) coupled to a triple quadrupole mass spectrometer (QTRAP 6500+, AB Sciex, Darmstadt, Germany) (Gläser et al., 2021a). Separation was conducted using a C18 column (Vision HT C18 HighLoad, 100 mm × 2 mm, 1.5 μm, Dr. Maisch, Ammerbuch-Entringen, Germany) at 45 °C, applying a linear gradient (0–7 min, 10% B to 90% B) of eluent B (0.1% formic acid in acetonitrile) against eluent A (0.1% formic acid in water) at a flow rate of 500 μL min⁻¹. Nybomycin was detected in the positive mode using selected ion monitoring of the $[M + H]^+$ adduct (m/z 299.1) (Rodriguez Estevez et al., 2018). Quantification was based on external standards (Cayman Chemical, Ann Arbor, USA).

2.10. Transcriptomics

Sample preparation and RNA sequencing were performed as previously described (Gläser et al., 2021a; Kuhl et al., 2020, 2021). In short, cells (1 mL broth) were collected by centrifugation (20,000×g, 4 °C, 1 min) and immediately frozen in liquid nitrogen. RNA was extracted with the Qiagen RNA Mini kit (Qiagen, Hilden, Germany) according to the manufacturer's instructions. Residual DNA was removed by digestion with 10 U RNase-free DNase I (Thermo Scientific) for 1 h in the presence of RiboLock RNase inhibitor (Thermo Scientific). After DNA digestion, the RNA was again purified with the same kit. The RNA quality was checked by Trinean Xpose (Trinean NV, Gentbrugge, Belgium) and Agilent RNA 6000 Nano Kit with an Agilent 2100 Bioanalyzer (Agilent Technologies, Böblingen, Germany). Ribosomal RNA (rRNA) was removed from total RNA with Ribo-Zero rRNA Removal Kit (illumina, San Diego, CA, USA), and removal of rRNA was checked using Agilent RNA 6000 Pico Kit and an Agilent 2100 Bioanalyzer (Agilent Technologies). cDNA libraries were prepared with TruSeq Stranded mRNA Library Prep Kit (illumina), and the resulting cDNA was paired-end sequenced using an illumina HiSeq 1500 system with a 2 × 75 bp read length. Reads were mapped to the *S. albidoflavus* J1074 genome sequence (CP059254.1) with Bowtie2 using standard settings (Langmead and Salzberg, 2012), except for increasing the maximal allowed distance for paired reads to 600 bases. For visualization of read alignments and raw read count calculation, ReadXplorer 2.2.3 was used (Hilker et al., 2014). For the resulting data, DESeq2 (Love et al., 2014) was used to QC the datasets via, for example, calculation of the sample-to-sample distances (Supplementary file 1, Fig. S2) and PCA (Supplementary file 1, Fig. S3). In addition, DESeq2 was employed to calculate DGE datasets. The raw datasets (sequenced reads) as well as processed datasets (input matrix & normalized read counts from DESeq2) are available from GEO (GSE240471). For statistical analysis, Student's *t*-test was carried out, and the data were filtered for genes with a log₂-fold change ≥ 1 (p value ≤ 0.05). Hierarchical clustering was conducted using the software package gplots (R core Team, 2014; Warnes et al., 2016). RNA extraction and sequencing were conducted in biological triplicate.

3. Results and discussion

3.1. Characterization of the nybomycin gene cluster through targeted gene inactivation identified all essential genetic elements for biosynthesis

As recently shown, transfer of the bacterial artificial chromosome (BAC) 4N24 containing the nybomycin gene cluster from *S. albidoflavus* subsp. *chlorinus* into the host *S. albidoflavus* Del14 enabled heterologous production of the compound in the new derivative *S. albidoflavus* 4N24 (Rodriguez Estevez et al., 2018). To elucidate which of the genes encoded in the transferred BAC 4N24 (Fig. 1A) are essential for

nybomycin biosynthesis, we performed a series of single gene deletions.

First, we individually deleted the genes *orf-01* to *orf-07* in strain 4N24. The sequences of *orf-01*, *orf-02*, *orf-03*, *orf-04*, and *orf-06* are predicted to encode hypothetical proteins, while *orf-05* putatively codes for an ATP-binding protein and *orf-07* for a streptomycin resistance protein (Rodríguez Estevez et al., 2018). We hypothesized that none of these seven genes participate in nybomycin biosynthesis. While this was confirmed for most of them, LC/MS analysis unexpectedly revealed that deletion of *orf-02* abolished production, indicating an important contribution of this gene to the biosynthetic pathway (Fig. 2A). BLAST analysis of the encoded protein sequence revealed 50% similarity to a putative transposase (A0A2TOGVF8) and, furthermore, the presence of an endonuclease domain (Pfam: PF13546), suggesting interaction of the Orf-02 protein with DNA structures. In conclusion, *orf-02* displays the new left boundary of the minimal cluster (Fig. 2B). In addition to *orf-01*, the next genes downstream of *orf-02* are *nybA*, *nybB*, and *nybC*, which

exhibit sequences homologous to the streptonigrin biosynthetic *stn* gene cluster (Rodríguez Estevez et al., 2018). Although the corresponding homologous *stn* genes presumably participate in streptonigrin biosynthesis, their specific function in this process remains unknown. To study the role of the three *nyb* genes, we inactivated their function. Nybomycin was not detected in extracts of 4N24 $\Delta nybA$ and 4N24 $\Delta nybC$, confirming that the encoded 3-carboxy-*cis*, *cis*-muconate cycloisomerase and NADPH: quinone reductase activities, respectively, are both essential (Fig. 2A). In contrast, deletion of *nybB*, encoding an FAD-binding protein, did not affect production, though reduced levels were detected (Fig. 2A). Further downstream, five genes are predicted to be nonessential: *nybV*, which putatively encodes a transporter of the major facilitator superfamily (MFS), *nybW*, *nybX*, and *nybZ*, predicted to encode transcriptional regulators, and *nybY*, encoding a hypothetical protein (Rodríguez Estevez et al., 2018). After individual gene inactivation, production of nybomycin was massively reduced in strains 4N24

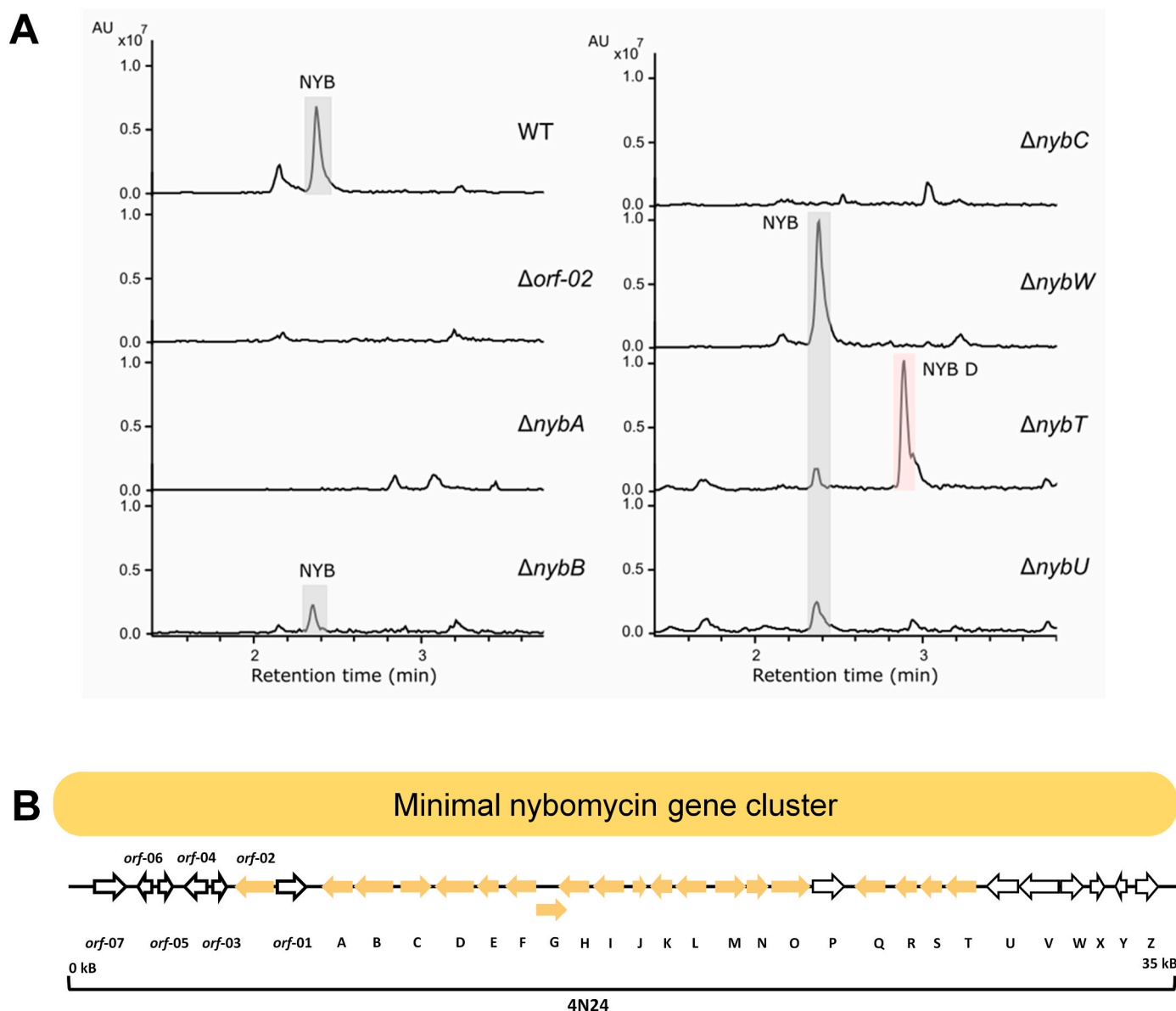


Fig. 2. Elucidation of gene function and identification of the minimal gene cluster for nybomycin biosynthesis in *S. albidoflavus* 4N24 using single gene deletion mutants. The data display LC–MS spectra of cultivation extract from *S. albidoflavus* 4N24 (WT) and the single gene deletion mutants $\Delta orf-02$, $\Delta nybA$, $\Delta nybB$, $\Delta nybC$, $\Delta nybW$, $\Delta nybT$, and $\Delta nybU$. The data represent the extracted ion chromatogram for m/z 299.10 \pm 0.1 Da (nybomycin) and m/z 285.1 \pm 0.1 Da (intermediate) (A). In addition, the newly identified minimal nybomycin gene cluster is shown (B). The genes from *orf-02* to *nybT*, except for *orf-01*, are essential for nybomycin biosynthesis.

$\Delta nybV$, 4N24 $\Delta nybX$, 4N24 $\Delta nybY$, and 4N24 $\Delta nybZ$ (Supplementary file 1, Fig. S4). In contrast, the 4N24 $\Delta nybW$ mutant produced slightly more nybomycin (Fig. 2A). Next, *nybU* and *nybT* were chosen for inactivation. The protein sequences of the two genes revealed high similarity (83%), and the encoded proteins were supposed to close the oxazoline ring during nybomycin biosynthesis (Fig. 1B). Both genes were predicted to code for isopenicillin N synthases (IPNS) which catalyze a chemically related thiazolidine ring closure during the synthesis of β -lactam antibiotics (Rodríguez Estevez et al., 2018). We observed weak production in both single-gene-deletion mutants (Fig. 2A). Interestingly, strain 4N24 $\Delta nybT$ accumulated a new derivative in addition to nybomycin. High-resolution LC-ESI/MS and UV analysis of the extracted culture supernatant indicated that the compound might be nybomycin D (Supplementary file 1, Fig. S5), a derivative that has been recently copurified from the culture broth of a *Streptomyces* coal mine isolate (Wang et al., 2019). The obvious homology between *nybT* and *NybU* suggest that inactivation of either IPNS function is complemented by the presence of the other, enabling biosynthesis in the corresponding single-gene-deletion mutants. This hypothesis was confirmed by the fact that a double-deletion mutant lacking both *nybT* and *nybU* no longer produced nybomycin (data not shown). Based on previous sequence analysis, it has been suggested that the genes from *nybA* to *nybZ* might constitute the nybomycin gene cluster (Rodríguez Estevez et al., 2018). Our experimental data allowed us to curate this picture. As shown, nybomycin synthesis requires the genes from *orf-02* to *nybT*, except for *orf-01* (Fig. 2B).

3.2. Mannitol-grown *S. albidoflavus* 4N24 accumulated up to 860 $\mu\text{g L}^{-1}$ nybomycin

As the starting point for strain development, we quantified nybomycin production in the original producer *S. albidoflavus* (*albus*) 4N24, which has been studied only qualitatively for production (Rodríguez Estevez et al., 2018). We used a minimal medium because it contains only one defined source of carbon, avoiding unresolvable cellular responses that would likely result from undefined complex medium ingredients (Schwechheimer et al., 2018a, 2018b) and facilitating elucidation of the planned metabolic engineering efforts (Gläser et al., 2021a).

Mannitol was chosen as the substrate because it enabled significantly higher product levels than glucose (Supplementary file 1, Fig. S6A, Fig. S6B), as observed in recent studies on oxytetracycline-producing *S. rimosus* (Beganovic et al., 2023). *S. albidoflavus* 4N24 formed 860 $\mu\text{g L}^{-1}$ nybomycin over 275 h (Fig. 3A). Once inoculated, the cells started to grow exponentially while consuming mannitol, ammonium, and phosphate. Within 24 h, the supplemented phosphate was depleted. The cell concentration increased further until mannitol was exhausted after 32 h, which then caused growth to stop. Interestingly, nybomycin was detectable during the growth phase, unlike most secondary metabolites, which are exclusively produced in the stationary phase (Kuhl et al., 2020; Ruiz et al., 2010; Seyedsayamdost, 2019). The start of production was likely triggered by the simultaneously occurring phosphate limitation (Gläser et al., 2021b). Taken together, 20% nybomycin was produced during the growth phase, though the stationary phase was the major phase of production (80%) (Fig. 3A).

3.3. P_{ermE^*} failed to drive nybomycin biosynthesis in engineered *S. albidoflavus* 4N24 due to a temporal mismatch between overexpressed target genes and product formation

The PP pathway and, further downstream, the SA pathway supply all carbon to form 2,6-diaminophenol, the centrepiece of nybomycin (Fig. 1B). In the first metabolic engineering step, we explored the potential of enhancing the precursor supply via the PP pathway. Two native PP pathway genes were selected for overexpression: *tkt* (encoding transketolase An in the reversible branch) and *zwf2* (encoding glucose 6-

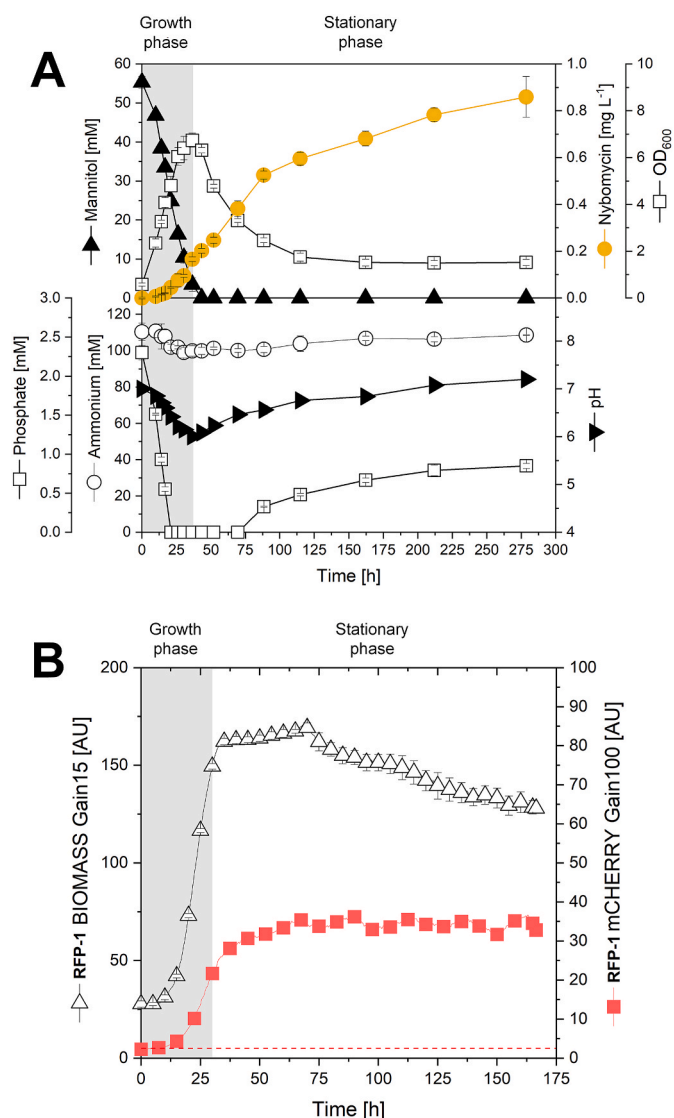


Fig. 3. Growth and nybomycin production in *S. albidoflavus* 4N24. The data comprise the cultivation profile in shake flasks on minimal mannitol medium (A) and the activity of the heterologous P_{ermE^*} promoter over time, assessed via a fluorescent reporter strain (*S. albidoflavus* 4N24 P_{ermE^*} mCherry) and online fluorescence monitoring using a miniaturized plate-based bioreactor (B). $n = 3$.

phosphate dehydrogenase in the oxidative branch) (Fig. 4A). Over-expression of each gene had previously proven to be efficient in (i) increasing the PP pathway flux in the actinobacterium *C. glutamicum* (Becker et al., 2007, 2011) and (ii) formation of PP pathway-based natural products, including violacein and deoxyviolacein in *E. coli* (Rodríguez et al., 2013) and FK506 in *S. sukubaensis* (Huang et al., 2013). In the present study, we separately integrated each gene under control of the constitutive promoter P_{ermE^*} (García-Gutiérrez et al., 2020) into the chromosome of *S. albidoflavus* 4N24, leading to strains NYB-1A (4N24 P_{ermE^*} *tkt*) and NYB-1B (4N24 P_{ermE^*} *zwf2*) (Fig. 4B). Neither of the two mutants, however, showed improved production: a nybomycin titer of 760 $\mu\text{g L}^{-1}$ for NYB-1A and 860 $\mu\text{g L}^{-1}$ for NYB-1B (Fig. 5A).

Next, we aimed to improve the flux through the SA pathway. To this end, we selected the *aroI*^{S187C} gene from *C. glutamicum* for heterologous expression (Fig. 4A). The gene encodes a feedback-resistant DAHP synthase (*aro* type-I DS) from the SA pathway, which has been successfully used to increase aromatic amino acid biosynthesis (Liao et al.,

Fig. 4. Metabolic pathway design to produce nybomycin in *Streptomyces albidoflavus* Del 14. The overview illustrates the targets of the stepwise metabolic engineering in primary and secondary metabolism (A) and the genetic layout of the NYB strain family over eleven generations of development created in this work (B). For each producer, we show the genetic changes. These comprised modifications to fuel precursor supply, i. e. the overexpression of native transketolase (*tkt*) and native glucose 6-phosphate dehydrogenase (*zwf2*) in the PP pathway, the deletion of phosphoenolpyruvate carboxylase (*ppc*) in the EMP pathway, the overexpression of heterologous DHAP synthase variants (*aroG*, *aroI*, *nybF*) in the shikimic acid pathway, and the overexpression of heterologous acetoacetyl-CoA synthase (*nybF*). In addition, the changes aimed to enhance assembly and export of the nybomycin molecule. These included overexpression of *nybM* and *nybV* as well as deletion of the regulator genes *nybW*, *nybX*, *nybY*, and *nybZ*. Promoters without labels refer to native promoters and genes already present in the genome. All changes were implemented stepwise into the chromosome of the basic nybomycin producer *S. albidoflavus* 4N24 that had been previously derived upon heterologous expression of the nybomycin gene cluster from *S. albus* subsp. *chlorinus* NRRL B-24108 (Rodriguez Estevez et al., 2018). It should be noticed that the best strain designs did not overexpress *nybM* and *nybV*, as these changes were detrimental to nybomycin production. Enlarged versions of the strain layouts are provided in Fig. S7 (strain generations 1 to 4) and Fig. S8 (strain generations 5 to 11) (Supplementary file 1). Further details on the genotype of the created strains are provided in Table 1.

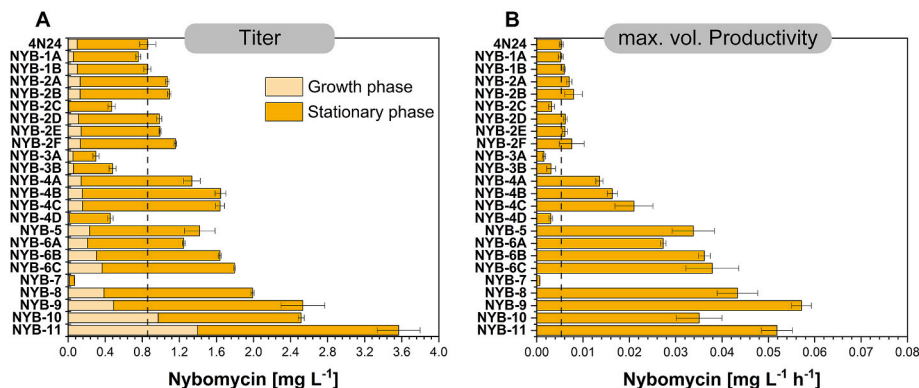


Fig. 5. Systems metabolic engineering of *Streptomyces albidoflavus* Del 14 for nybomycin production. During strain development, the production performance of the created producers was evaluated on minimal medium with 10 g L⁻¹ mannitol as the sole source of carbon. The data display the final nybomycin titre (A), whereby the fraction of product synthesized during the growth phase (pale orange) and the stationary phase (bright orange) is indicated. In addition, the maximum volumetric nybomycin productivity observed during the process is shown (B). n = 3.

2001). The constructed strain NYB-1C (4N24 P_{ermE^*} *aroI*^{S187C}) (Fig. 4B), however, did not differ in nybomycin production (data not shown). There are two possibilities to explain the somewhat surprising lack of improvement in the three strains: (i) the target genes were insufficiently expressed and/or (ii) nybomycin formation was not limited by precursor supply. P_{ermE^*} represents a well-known promoter that has been successfully used many times to drive gene expression in *Streptomyces* (Chen et al., 2012; Huo et al., 2012; Kallifidas et al., 2018; Lu et al., 2016; Ma et al., 2020; Mo et al., 2019; van Wezel et al., 2000). However, as promoters can vary in strength depending on the conditions and appropriate promoter functionality is crucial for successful strain engineering, we experimentally benchmarked P_{ermE^*} .

For this purpose, we constructed the reporter strain *S. albidoflavus* RFP-1 (4N24 P_{ermE^*} *mCherry*) (Table 1, Fig. 7A). The construct was integrated into the chromosome using the phiBT1 integration site, resulting in expression of mCherry under control of P_{ermE^*} . For integration, we used the same locus as for the genetic targets shown above. Most previous studies on promoter strength in *Streptomyces* have relied on endpoint measurement of expression (Bibb et al., 1994; Seghezzi et al., 2011; Siegl et al., 2013). However, as *S. albidoflavus* exhibited distinct dynamics in nybomycin production (Fig. 3A), we decided to measure gene expression dynamically. The obtained reporter strain was therefore analyzed online for growth and fluorescence (Kohlstedt et al., 2018). Interestingly, mCherry was exclusively expressed during the first 40 h of cultivation, the growth phase (Figs. 3B, 7B and 7C). The fluorescence signal remained unchanged during the entire stationary phase, revealing a previously overlooked dependence of P_{ermE^*} activity on the growth status of *S. albidoflavus* (Myronovskiy and Luzhetskyy, 2016). In terms of nybomycin production, the dynamics of P_{ermE^*} activity were highly unfavorable. Use of this promoter did not allow the desired overexpression of target genes during the major phase of production, in which the encoded activity would be needed.

3.4. Time-resolved fluorescence analysis revealed differences in promoter dynamics and identified P_{kasOP^*} and P_{SP41} as optimal synthetic control elements

In the next step, we searched for superior promoters to drive production-coupled gene expression. Seven alternative promoters were selected: the thiostrepton-inducible promoter P_{tipA} conferring substantial uninduced activity (Myronovskiy and Luzhetskyy, 2016), the mutagenized P_{ermE^*} derivative P_{21} (Siegl et al., 2013), the constitutive phage-derived promoter P_{SF14} (Labes et al., 1997) and the deregulated promoter variant P_{kasOP^*} and its synthetic derivatives P_{SP41} , P_{SP43} , and P_{SP44} (Bai et al., 2015) (Fig. 7A). Each promoter was cloned in front of *mCherry*, and the respective plasmids were integrated into *S. albidoflavus*, yielding the reporter strains RFP-2 to RFP-8 (Fig. 7A, Table 1). The promoters differed strongly in their dynamic expression pattern (Fig. 7B and C). P_{tipA} appeared inactive throughout the entire culture, indicating that its uninduced activity was not significant, in contrast to previous observations (Myronovskiy and Luzhetskyy, 2016). P_{SF14} was found to be weaker than P_{ermE^*} , the opposite of what had been observed in *S. lividans* (Labes et al., 1997), underlining the importance of case-specific evaluation. P_{21} was as strong as P_{ermE^*} . The activity of P_{21} and P_{SF14} was almost entirely restricted to the growth phase. None of these alternative promoters appeared useful to drive precursor supply for nybomycin production.

This picture completely changed when analyzing the four P_{kasOP^*} -based promoters. The two variants P_{SP43} and P_{SP44} were found to be threefold more active than P_{ermE^*} based on final fluorescence (Fig. 7B and C). P_{kasOP^*} and its synthetic derivative P_{SP41} were the two best promoters, exhibiting the highest overall activity (sevenfold higher than P_{ermE^*}) and, importantly, consistently high expression throughout the culture process, including the stationary phase, during which most nybomycin was produced.

3.5. Second-generation producers with increased flux through the PP and SA pathways exhibited up to 50% increased nybomycin productivity

The best promoter, P_{kasOP^*} , was used to overexpress *tkf* and *zwf2* to enhance the supply of the PP pathway intermediate E4P (Fig. 4B). Encouragingly, the two mutants NYB-2A (4N24 P_{kasOP^*} *tkf*) and NYB-2B (4N24 P_{kasOP^*} *zwf2*) accumulated 29% and 31% more nybomycin than the parent strain, i.e., 1070 and 1095 $\mu\text{g L}^{-1}$, respectively (Fig. 5A). At the same time, the maximum specific nybomycin production rate was increased up to 50% (Fig. 5B). This improvement is important in two aspects: it revealed that synthesis of nybomycin was limited by the supply of its central carbon moiety and indicated the high value of P_{kasOP^*} for tailored gene expression of production-supporting genes.

Next, DAHP synthase (DS) emerged as a relevant point of control (Fig. 1B) (Sander et al., 2019), given its impact on formation of SA pathway-based products, such as salivianic acid (Yao et al., 2013), violacein (Rodrigues et al., 2013), caffeic acid (Zhang and Stephanopoulos, 2013), and avenanthramides (Eudes et al., 2013). To overcome a potential limitation at this step, we used P_{kasOP^*} to express genes from two different donors that encoded feedback-resistant variants of the enzyme: *aroG*^{D146N} from *E. coli* (Kikuchi et al., 1997) and *aroI*^{S187C} from *C. glutamicum* (Liao et al., 2001) (Fig. 4B). Beneficially, a 20% higher nybomycin titer (Fig. 5A) and a 15% increased productivity (Fig. 5B) were achieved in the new mutants NYB-2D (4N24 *aroG*^{D146N}) and NYB-2E (4N24 *aroI*^{S187C}).

Interestingly, the *nyb* cluster itself also comprises a DS-encoding gene, namely, *nybF*. Overexpressing this gene resulted in a further increased titer (1160 $\mu\text{g L}^{-1}$) in the new strain NYB-2F (Fig. 5A). Moreover, volumetric productivity was increased by 40% (Fig. 5B). The exact reason for the additional improvement is not clear. Eventually, the GC-rich *nybF* gene (75%) enabled increased expression due to its more suitable codon usage (Rohles et al., 2022; Weiland et al., 2023) and/or the NybF protein exhibited superior kinetics, but more work is needed to explore this issue further.

Obviously, NybF differs substantially from the other enzymes. Aligned amino acid sequences revealed 52% identity between AroG and Aro I (95% coverage), with almost no conserved regions detected in NybF (Supplementary file 1, Fig. S9A). *C. glutamicum* possesses another DAHP synthase, denoted Aro II (NCgl 2098) (Ikeda, 2006), a plant-like type II DAHP synthase (Walker et al., 1996). NybF revealed 37% similarity to Aro II (91% coverage) (Supplementary file 1, Fig. S9B). To date, metabolic engineering for production of aromatic amino acids and related derivatives has commonly involved recruiting type I feedback-resistant enzyme variants from *E. coli* (AroG, AroF, AroH) or *C. glutamicum* (Aro I) (Rodriguez et al., 2014), whereas it seems that type II enzymes have been largely neglected. Based on our findings, however, type II DAHP synthases seem to deserve a closer look for future metabolic and enzyme engineering to overproduce aromatic amino acids and related derivatives.

Next, we aimed to redirect PEP from the EMP pathway toward nybomycin (Fig. 1B). To this end, the gene *ppc*, coding for PEP-consuming phosphoenolpyruvate carboxylase, was deleted in frame, resulting in strain NYB-2C (4N24 Δ *ppc*). The deletion strain, however, needed almost 100 h to reach the maximum cell concentration (Supplementary file 1, Fig. S10A) while producing almost twofold less nybomycin (470 $\mu\text{g L}^{-1}$) (Fig. 5A). When NYB-2C was grown in complex DNP medium, the growth retardation was partially recovered, but nybomycin production remained far below that of the parent strain (Supplementary file 1, Fig. S11). It has been reported that a Δ *ppc* mutant of *Corynebacterium glutamicum* is affected in growth on minimal medium (Peters-Wendisch et al., 1993). In addition, the deletion of *ppc* in *S. tsukubaensis* affects growth on complex medium only slightly (Huang et al., 2013) but enables increased production of FK506 (built from chorismic acid as a precursor) (Huang et al., 2013).

Genetically, the three strains, like other microbes, comprise the same set of enzymes around the pyruvate node, namely, pyruvate

carboxylase, phosphoenolpyruvate carboxylase, pyruvate kinase, phosphoenolpyruvate carboxykinase, and malic enzyme, offering the same options to redirect fluxes upon genetic perturbation (Becker et al., 2008; Meza et al., 2012; Huang et al., 2013). A possible explanation for the different behavior is the carbon sources used, i.e., mannitol on the one hand (this work) and glucose on the other (Peters-Wendisch et al., 1993). Mannitol-grown actinobacteria exhibit a highly different intracellular flux distribution from glucose-grown actinobacteria (Hoffmann et al., 2018, 2021) and, therefore, might respond differently to the absence of *ppc*. Indeed, NYB-2C produced 15% more nybomycin than its parent strain 4N24 when grown on glucose (Supplementary file 1, Figs. S6C and S6D), showing the opposite effect of mannitol-grown cells. However, none of the glucose-based cultures reached the nybomycin level achieved by 4N24 on mannitol. More work is needed in the future to better understand these substrate-related effects.

3.6. Selective metabolic engineering of different steps of the nybomycin pathway resulted in strains with poor growth and low production

Next, we focused on the nybomycin biosynthetic pathway. Inspired by the fact that nybomycin production could be driven by enhanced precursor supply (Fig. 5A and B), we overexpressed *nybM*, a gene encoding acetoacetyl-CoA synthase, which supplies two acetoacetyl-CoA residues to assemble the nybomycin core (Figs. 1B and 4A). The created strain NYB-3A (4N24 P_{kasOP^*} *nybM*), however, produced only 300 $\mu\text{g L}^{-1}$ of the antibiotic, almost threefold less than the natural producer (Fig. 5A). Furthermore, the mutant was heavily impaired in vitality (Supplementary file 1, Fig. S10B). Overexpression of acetoacetyl-CoA synthase in *Saccharomyces cerevisiae* results in a similar phenotype, as the mutation did not increase (acetoacetyl-CoA-based) sesquiterpene production, and it was concluded that the advanced supply of acetoacetyl-CoA stimulated its thiolysis and resulted in a futile cycle (Tippmann et al., 2017). In this regard, acetoacetyl-CoA synthase overexpression in NYB-3A might have affected the availability of malonyl-CoA, a key precursor of native fatty acid biosynthesis that requires fine-tuned balancing to avoid limiting and even toxic effects (Pizer et al., 2000).

Furthermore, the nybomycin cluster contains *nybV*, encoding a putative transporter. As shown, deletion of this gene reduced nybomycin formation in *S. albidoflavus* 4N24 (Fig. 2A). Therefore, we aimed to enhance product export. To this end, the *nybV*-overexpressing strain NYB-3B was generated (4N24 P_{kasOP^*} *nybV*). However, the transporter mutant showed weak growth (Supplementary file 1, Fig. S10C) and low nybomycin production (Fig. 5A). This finding differed from previous results that achieved increased production of tetracycline (Yin et al., 2017), pristnamycin (Jin et al., 2010), and avermectin (Qiu et al., 2011) in strains with increased export capacity.

3.7. The combination of beneficial targets streamlined precursor supply and provided fourth-generation cell factories with elevated nybomycin titers

Individual overexpression of the native genes *tkf* and *zwf2* and the heterologous genes *aroG*^{D146N} (*E. coli*), *aroI*^{S187C} (*C. glutamicum*), and *nybF* (*S. albidoflavus* subsp. *chlorinus*) enhanced nybomycin production. We hypothesized that a combination of beneficial targets might enable further improvement. We focused on complementary combinations of *tkf*, *zwf2*, and *nybF* and created double and triple combinations, yielding strains NYB-4A (P_{kasOP^*} *tkf* *zwf2*), NYB-4B (P_{kasOP^*} *nybF* *zwf2*), NYB-4C (P_{kasOP^*} *nybF* *tkf*), and NYB-4D (P_{kasOP^*} *nybF* *tkf* *zwf2*) (Fig. 4B). The double-combination mutants exhibited improvements in titer and productivity. Coexpression of *nybF* with a PP pathway gene was most successful, resulting in almost twofold more nybomycin in strains NYB-4B (1644 $\mu\text{g L}^{-1}$) and NYB-4C (1638 $\mu\text{g L}^{-1}$) compared to the basic producer (Fig. 5A). The corresponding increase in maximum productivity was threefold (NYB-4B) and fourfold (NYB-4C) (Fig. 5B). Notably, the

combinatorial effects for the two strains were more than additive. For example, the titer increase for the NYB-4B strain was more than 50% higher (+779 $\mu\text{g L}^{-1}$) than the sum of the increase observed for the single overexpression strains (+511 $\mu\text{g L}^{-1}$). Surprisingly, the triple mutant (NYB-4D) that overexpressed *nybF*, *tkl* and *zwf2* revealed weak performance (Fig. 5A) and was even less efficient than the basic

producer, though its growth was unchanged. Evidently, the combined effects were too strong and caused an imbalance in metabolism. Similarly, previous metabolic engineering efforts have caused unforeseen effects on antibiotic formation and sporulation in *S. lividans* due to high intracellular NADPH levels (Jin et al., 2017).

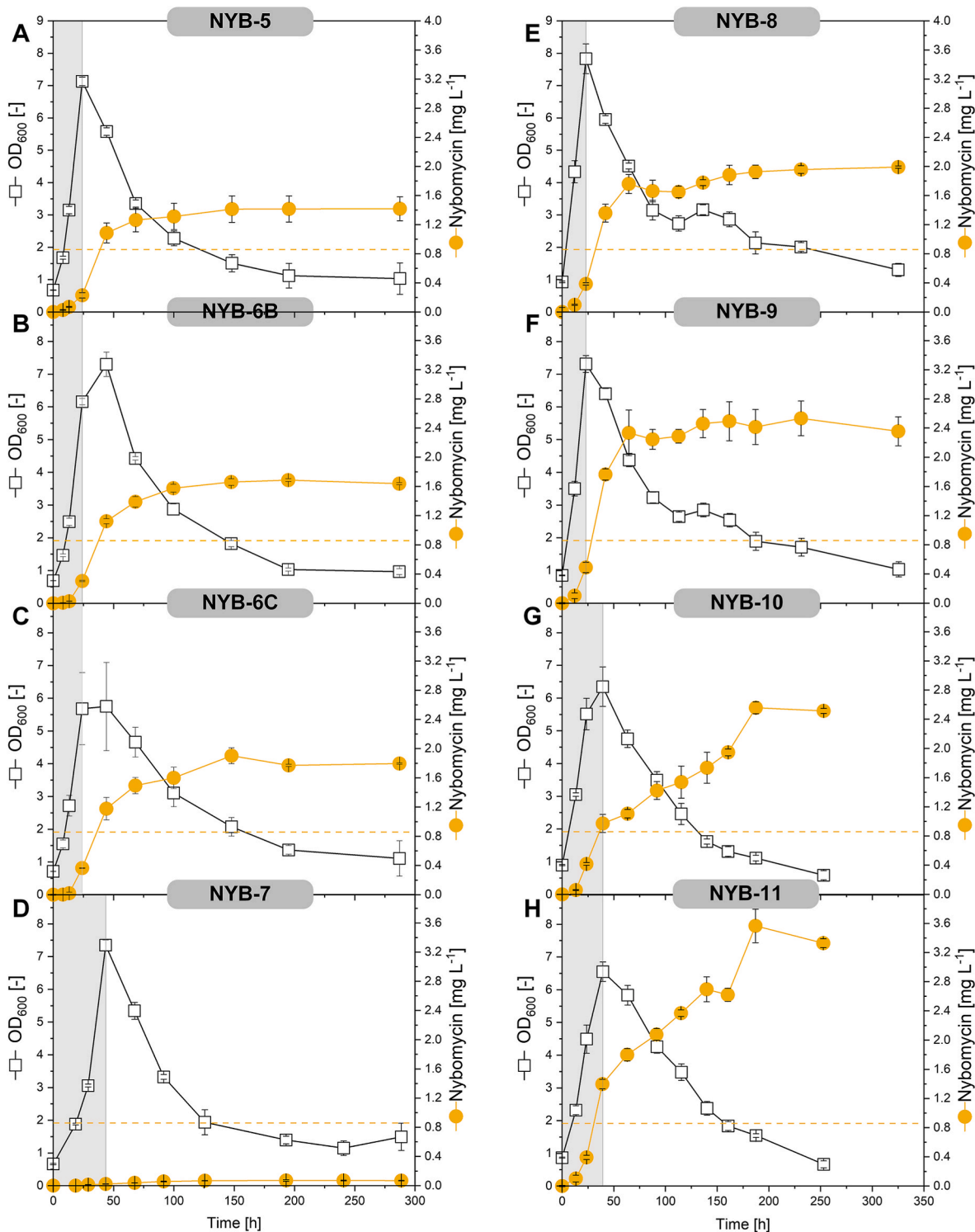


Fig. 6. Growth and nybomycin production in advanced nybomycin cell factories. The data comprise the cultivation profiles of strains *Streptomyces albidoflavus* NYB-5 (A), NYB-6B (B), NYB-6C (C), NYB-7 (D), NYB-8 (E), NYB-9 (F), NYB-10 (G), and NYB-11 (H). For comparison, the orange dotted line in each plot shows the maximum titer of the basic producer 4N24 (Fig. 3A). All strains were grown in shake flasks on minimal mannitol medium. The corresponding genetic layouts are given in Fig. 4 and Table 1. n = 3.

3.8. Deletion of *nybW* decoupled production from the growth state of *S. albidoflavus* and boosted volumetric productivity in fifth- and sixth-generation strains

Metabolic engineering efforts directed to individual steps of the terminal assembly of nybomycin failed to provide higher levels of the product (Figs. 2, Fig. 4, Fig. 5). We hypothesized that the nybomycin pathway might require balanced expression of its different genes to achieve increased flux, as previously observed during metabolic engineering of other microbial biosynthetic routes (Giesselmann et al., 2019; Jones et al., 2015; Schwentner et al., 2019). For coordinated activation, biosynthesis-related gene clusters for natural products typically contain specific regulator genes (Bednarz et al., 2019; Liu et al., 2013), and removal of such regulatory elements has been found to be helpful in

overproducing daptomycin (Mao et al., 2017) and chromomycin (Sun et al., 2018).

Based on sequence homology, *nybW* has been suggested as a potential regulatory element of the nybomycin pathway (Rodríguez Estevez et al., 2018). Interestingly, deletion of *nybW* slightly improved nybomycin production during qualitative inspection for functional characterization of the cluster (Fig. 2A). Therefore, we decided to construct the regulator-deficient mutant *S. albidoflavus* NYB-5 (4N24 Δ *nybW*) (Fig. 4B). When grown on minimal mannitol medium, strain NYB-5 produced a nybomycin titer of 1418 $\mu\text{g L}^{-1}$, 70% more than the basic strain (Figs. 5A and 6A). It also grew well, indicating that the genetic modification did not interfere with vitality. The greatest change in the mutant, however, was accelerated production. Nybomycin formation began earlier, while the cells were still growing, resulting in a

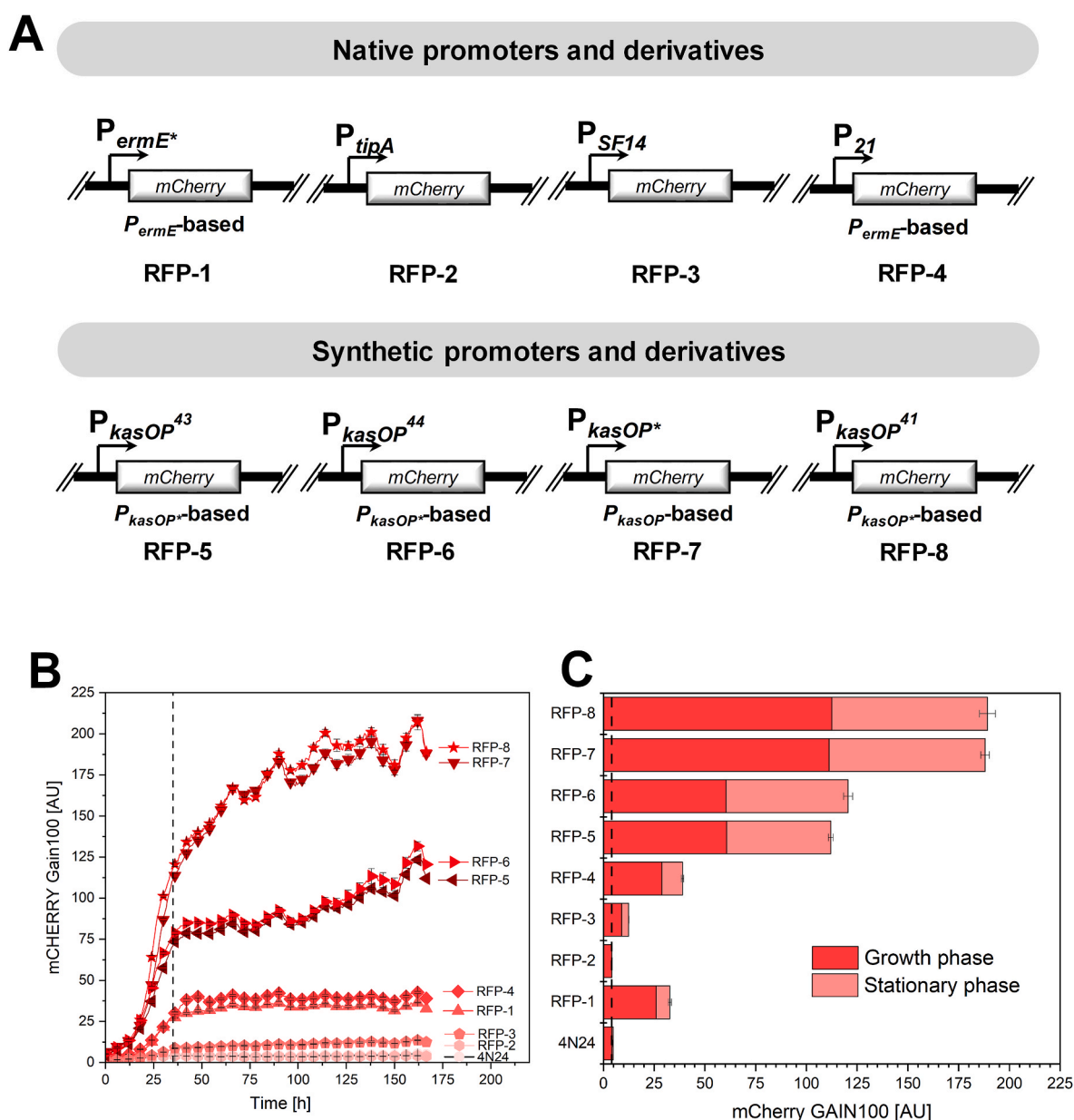


Fig. 7. Evaluation of heterologous promoters for expression efficiency in *S. albidoflavus* 4N24. Each promoter was benchmarked using a fluorescent reporter strain and online sensing of fluorescence. A set of eight promoters was tested, including four native and four synthetic variants. MCherry was used as reporter protein in each case (A). Each reporter strain was studied for the dynamics of expression on minimal mannitol medium in a miniaturized plate-based bioreactor with online fluorescence sensing (B). The dashed vertical line indicates the end of the growth phase and the beginning of the stationary phase (B). The two phases were identified from the growth behavior of the strains. The data were used to infer the relative expression strength during growth (pale red colour) and the stationary phase (strong red colour) (C). $n = 3$.

production rate higher than that of all other strains (Fig. 5B). While the basic strain produced nybomycin mainly in the stationary phase, the regulator mutant accumulated the product in both phases, regardless of the growth state (Fig. 6A). The maximum titer could therefore be reached after 125 h, shortening the overall process.

Subsequently, the $\Delta nybW$ mutation was combined with the other beneficial targets. A set of sixth-generation producers was constructed, comprising three-target combinations, i.e., NYB-6A (4N24 $\Delta nybW P_{kasOP^*} nybF zwf2$), NYB-6B (4N24 $\Delta nybW P_{kasOP^*} nybF tkt$), and NYB-6C ($\Delta nybW P_{kasOP^*} tkt zwf2$). The $\Delta nybW$ modification modestly increased productivity in all strains, revealing beneficial synergetic effects of the targets (Fig. 5B). Thus, strains NYB-6B and NYB-6C achieved the highest titers (Figs. 5A, 6B and 6C). All three mutants showed a favorable growth state-decoupled production phenotype. We also constructed a quadruple mutant, namely, NYB-7 (4N24 $\Delta nybW P_{kasOP^*} nybF tkt zwf2$). Nybomycin production in this strain, however, was almost eliminated ($70 \mu\text{g L}^{-1}$) (Fig. 6D). Obviously, the growth deficiency of the parent strain NYB-4D could not be rescued by deletion of the regulator. Taken together, systems metabolic engineering of *S. albidoflavus* 4N24 through several cycles of optimization substantially enhanced nybomycin production. In comparison to the basic strain, the two best producers, NYB-6B and NYB-6C, produced the reverse antibiotic at an almost twofold higher titer and up to sevenfold higher productivity.

3.9. In an optimized process, *S. albidoflavus* NYB-6B formed up to 7.2 mg L^{-1} nybomycin

S. albidoflavus NYB-6B was chosen to benchmark the achieved performance. First, we used dextrin-based DNPM medium, a complex mixture that is commonly chosen for natural product formation in *Streptomyces* (Ahmed et al., 2020; Estevez et al., 2020; Paulus et al., 2022), including production of nybomycin in *S. albidoflavus* 4N24 (Rodríguez Estevez et al., 2018). When grown on a formulation with 40 g L^{-1} dextrin (DPNM 40), the NYB-6B overproducer produced 4.1 mg L^{-1} nybomycin, almost 60% more than the basic strain (Supplementary file 1, Fig. S12). Interestingly, production mainly occurred during the initial growth phase. Use of an increased dextrin level (75 g L^{-1}) resulted in prolonged production and a final nybomycin titer of 5.5 mg L^{-1} . Next, we studied the strain on the minimal medium formulation with increased initial mannitol (25 g L^{-1} , 50 g L^{-1} , 75 g L^{-1}) and phosphate (1.0 g L^{-1} , 2.0 g L^{-1} , 3.0 g L^{-1}) levels (Supplementary file 1, Fig. S13). The recombinant strain performed well in all setups and produced a final nybomycin titer of 7.2 mg L^{-1} ($7185 \mu\text{g L}^{-1}$) for the highest substrate level tested, reflecting an overall 8.3-fold improvement in production. The higher the initial concentration of mannitol was, the longer nybomycin production was sustained and the higher the final titer was. As the growth of the cells was slightly delayed when using 75 g L^{-1} mannitol, production required approximately 200 h. At 25 and 50 g L^{-1} mannitol, growth was not affected, and biomass was built up quickly until the mannitol was completely consumed. Accordingly, the maximum titer was reached earlier, resulting in a substantially higher maximum productivity. Notably, in all cases, the product was formed in the presence of phosphate; thus, deregulated cluster expression enabled this superior production phenotype.

3.10. During the production phase, *S. albidoflavus* 4N24 upregulated various routes for acetyl-CoA supply but downregulated shikimate and nybomycin biosynthesis

Next, we conducted RNA sequencing of *S. albidoflavus* 4N24 to shed light on the changes related to the shift from growth (13 h) to nybomycin production (70 h) (Fig. 3A), given the highly informative value of transcriptomic data in evaluating genetically and environmentally perturbed strains (Kohlstedt et al., 2014, 2022; Schilling et al., 2007). Expression of 2044 of 5790 encoded genes (35.3%) significantly differed between the growth and production phases (\log_2 -fold change ≥ 1 , $p \leq$

0.05), with 868 genes downregulated and 1176 genes upregulated.

Regarding the high-flux pathways of carbon core metabolism, precursor supply, and nybomycin biosynthesis, the analysis provided important insights (Fig. 8). As predicted from depletion of mannitol and cessation of growth, genes encoding mannitol import and metabolism (up to \log_2 -fold 5.7), the EMP pathway, and most TCA cycle enzymes were downregulated during the stationary phase. This picture matches those of related strains (Hwang et al., 2019; Lee et al., 2022). An interesting exception was upregulation of genes encoding succinate dehydrogenase complex II (5662, 5663, and 5664) and upstream conversion of L-glutamate to succinate. The succinate dehydrogenase complex has a unique dual function in that it converts succinate to fumarate in the TCA cycle and channels electrons to the respiratory chain (Huang and Millar, 2013; Park et al., 1995), thereby preventing production of superoxide anion (O_2^-), a reactive oxygen species (Dalla Pozza et al., 2020; Hwang et al., 2014). Ultimately, its upregulation is linked to protection. Furthermore, the cells activated catabolic routes for degradation of branched-chain amino acids (L-valine, L-leucine, L-isoleucine) and lipids (\log_2 -fold up to 5.7), eventually mobilizing internal carbon (Gläser et al., 2021a) (Fig. 8, Supplementary file 1, Fig. S14). Notably, these pathways yielded acetyl-CoA as a central intermediate (Fujita et al., 2007; Kaiser and Heinrichs, 2018; Massey et al., 1976; Pavoncello et al., 2022). In addition, the cells showed upregulation of routes to synthesize acetoacetyl-CoA from acetyl-CoA. Nybomycin biosynthesis needed CoA-based carbon such that, overall, the activated acetyl-CoA supply appeared favorable and was ultimately sufficient. This at least explains why overexpression of *nybM* did not provide any improvement in production. In terms of precursor supply, however, genes encoding enzymes of the PP pathway and the shikimate and chorismate routes showed reduced expression during the production phase (Fig. 8), presumably limiting the supply of 4-aminoanthranilate for nybomycin biosynthesis (Fig. 1B). In this regard, overexpression of *zwf* and *tkt*, as well as the DAHP-encoding variants *aroG*^{D146N}, *aroF*^{S187C}, and *nybF*, respectively, appeared to be a good choice to overcome the naturally occurring downregulation.

The expression pattern of the nybomycin cluster, which was inspected next, was very surprising. The cluster was highly expressed during the growth phase and greatly downregulated during the major nybomycin production phase. During the major production phase, almost all cluster genes showed reduced expression (\log_2 -fold changes up to -3.4), except for *nybV*, encoding the nybomycin exporter, and the putative regulators *nybX*, *nybZ*, and *nybY*. This behavior appeared extremely unfavorable in terms of production performance. Typically, BGCs are activated when cells enter the stationary phase and begin producing natural products, which is regarded as an important feature for high-level production (Bobek et al., 2021; Gramajo et al., 1993; Holt et al., 1992; Kormanec et al., 2014; Novakova et al., 2022; Zhu et al., 2022). Regarding global regulation, genes encoding sigma factors and presumed regulators revealed complex changes over time, which mirrored the picture observed for other *S. albidoflavus* Del14 derivatives when shifting from growth to the stationary phase (Supplementary file 1, Table S2).

3.11. Advanced producers exhibited an even stronger transcriptional downregulation of the nybomycin pathway during the stationary phase

Next, we compared the transcriptomes of different producers to trace the effects that resulted from successive rounds of strain engineering (Fig. 9). To this end, we analyzed three differently performing *zwf*-based mutants: NYB-2B (*zwf*), NYB-4B (*nybF zwf*), and NYB-6B ($\Delta nybW nybF zwf$). We also examined the *tkt*-based derivative NYB-6C ($\Delta nybW nybF tkt$), but it was almost identical to NYB-6B, except for the two differently engineered genes. In general, targeted genes (*nybF*, *zwf* and *tkt*) were found to be strongly overexpressed during the growth and production phases, revealing that (i) the P_{kasOP^*} promoter reliably enabled increased expression and (ii) the genetic modifications indeed increased

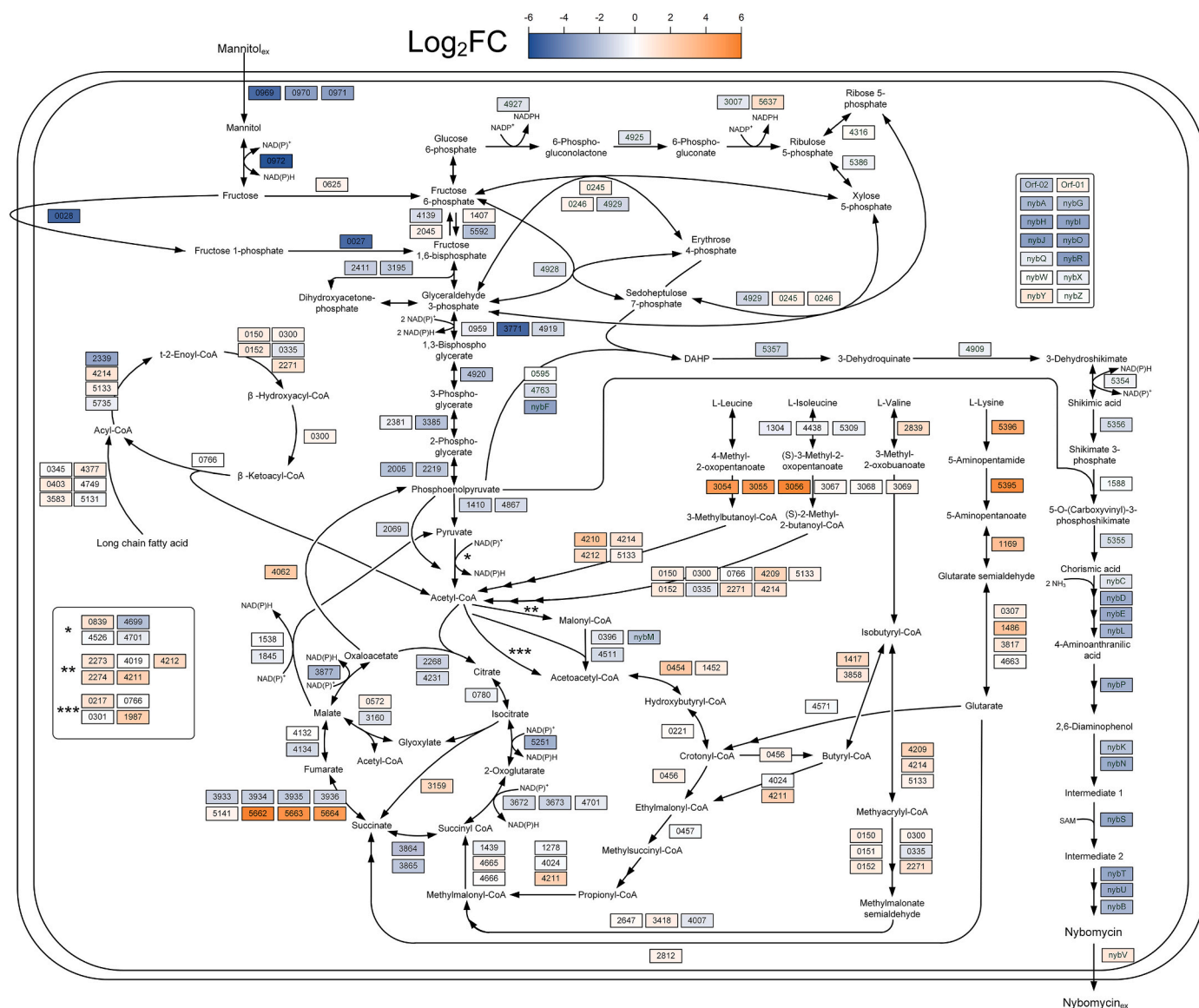


Fig. 8. Dynamic gene expression changes in the basic nybomycin producer *S. albidoflavus* 4N24. The data reflect expression differences between the growth phase (13 h, used as reference) and the major nybomycin production phase (70 h) and include genes encoding enzymes of major catabolic and anabolic pathways, nybomycin biosynthesis, and precursor supply. Enzymes were assigned to certain reactions based on KEGG pathway maps and gene annotations obtained during RNA sequencing. The numbers in the boxes correspond to the locus tags in the sequence of the chromosome of *Streptomyces albidoflavus* J1074 D14 4N24 (Accession no. CP113229). For all samples, the biological replicates clustered closely, indicating excellent data quality (Supplementary file 1, Fig. S2, Fig. S3). n = 3.

nybomycin production. Based on these findings, we recommend the synthetic *P*_{KasOP*} promoter and its derivatives (Fig. 7) for metabolic engineering efforts in *S. albidoflavus* and related strains (Ahmed et al., 2020), which require growth-independent constitutive overexpression of target genes.

Notably, deletion of *nybW* increased expression of several upstream cluster genes, namely, *nybQRSTUV*, though the increase for *nybUV* was much higher than that of the other genes (Fig. 9B). Within the cluster, the *nybQRSTUV* genes are transcribed in the same direction (Fig. 1A), and we conclude their expression to be under control of the NybW repressor.

However, the expression data of the other 18 cluster genes during the major production phase were surprising. Compared to the basic producer, the strains NYB-4B, NYB-6B, and NYB-6C exhibited strong downregulation of these genes. This change indicated a serious bottleneck, limiting production. All advanced strains, for unknown reasons, exhibited slightly elevated expression of *nybXYZ*, encoding two regulators (*nybX*, *nybZ*) and a small protein (87 AA) of unknown function

(Fig. 1A). Considering that the regulators are presumably repressors, their upregulation might have indeed caused the observed downregulation of most of the cluster genes, i.e., all genes that were not controlled by *nybW*. Interestingly, the single-gene-deletion strains *nybX*, *nybY*, and *nybZ* exhibited reduced nybomycin titers, which initially seemed to rule out elimination of the regulatory genes as a target for optimization (Supplementary file 1, Fig. S4). The expression dynamics, however, indicated that the regulators acted together or depended on each other, such that the remaining repressor genes in the single-gene-deletion mutants could still repress the cluster.

On the other hand, the genetic modifications of primary metabolism affected expression of the correspondingly chosen target gene rather locally but did not cause broader effects, e.g., within the EMP and PP pathways, the TCA cycle, and related routes (Fig. 9C, D, Fig. 9E and F). This observation implies that genes encoding enzymes upstream or downstream of the modified step in the corresponding pathway were sufficiently expressed to enable increased flux.

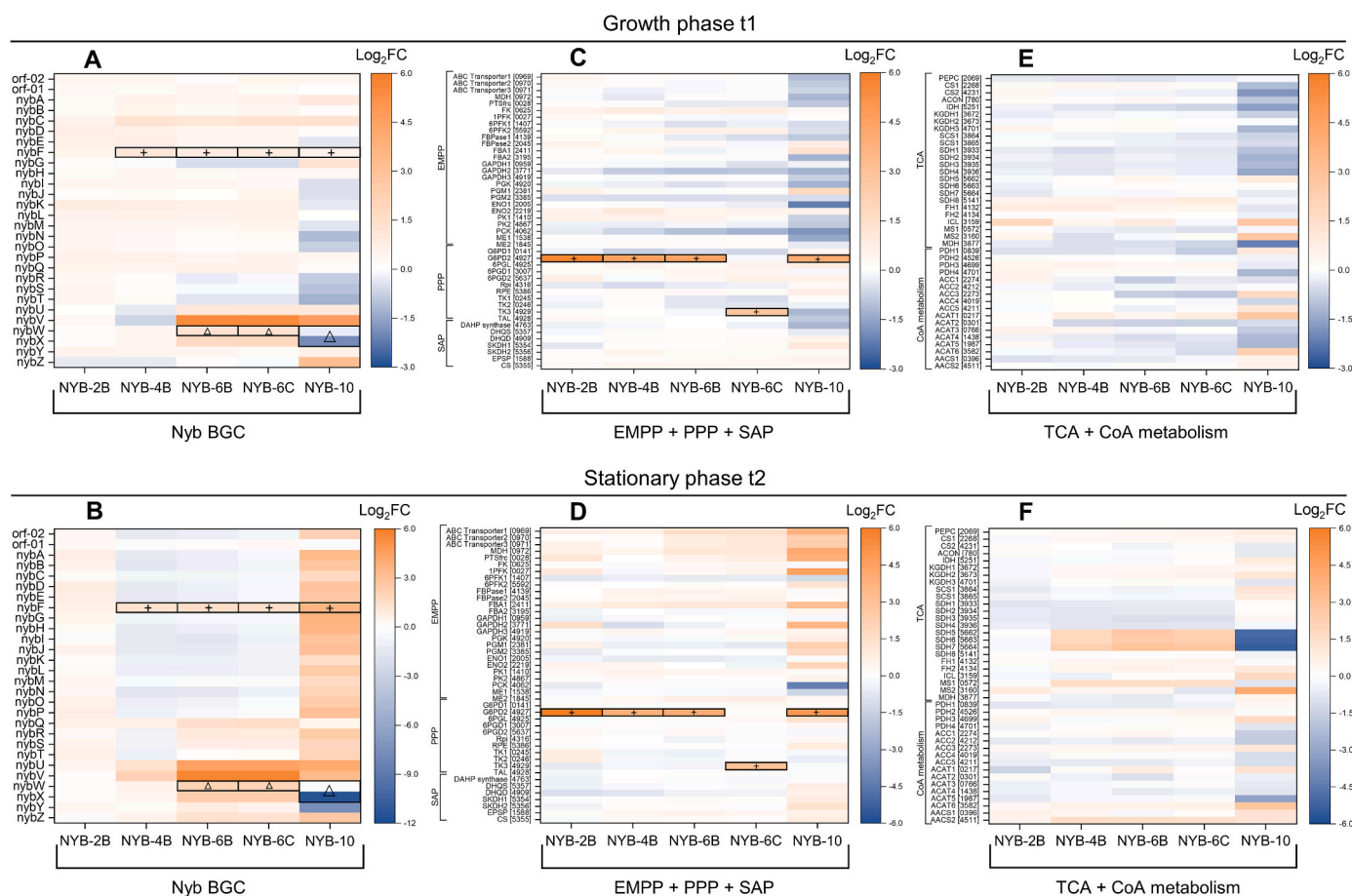


Fig. 9. Gene expression in different mutants of *S. albidoflavus* 4N24, metabolically engineered for nybomycin overproduction. The data reflect differences between strains 4N24, NYB-2B, NYB-4B, NYM-6B, and NYB-6C during the growth phase (13 h) and the major nybomycin production phase (70 h). The data for the basic producer 4N24, analyzed after 13 h, are used as a reference. The displayed genes include nybomycin biosynthesis (A, D), the Emden-Meyerhof-Parnas (EMP), the pentose phosphate (PP), and the shikimic acid (SA) pathways (B, E), as well as the TCA cycle and the reactions linked to the metabolism of CoA thioesters (C, F). Enzymes were assigned to certain reactions based on KEGG pathway maps and gene annotations obtained during RNA sequencing. One should note that (in the corresponding strains NYB6B and NYB-6C) *nybW* was only partially deleted without affecting its promoter region to exclude neighbouring effects. The detected *nybW* expression in NYB-6B and NYB-6C therefore proved the sustained activity of the promoter but did not reflect the expression of a functional NybW protein. n = 3.

3.12. The combinatorial engineering of primary and secondary metabolism maximized nybomycin production in tenth- and eleventh-generation strains

To elucidate control of the cluster, we decided to engineer its regulatory part in strain 4N24. Therefore, we replaced the genes *nybWX* and *nybWXYZ* with a kanamycin resistance gene. The new strains NYB-8 (4N24 $\Delta nybWX$) and NYB-9 (4N24 $\Delta nybWXYZ$) were grown in mannitol minimal medium after verifying the correctness of the introduced mutations by PCR and sequencing. NYB-8 accumulated 1990 $\mu\text{g L}^{-1}$ nybomycin (Fig. 6E), while NYB-9 formed 2530 $\mu\text{g L}^{-1}$ (Fig. 6F), up to threefold more than the basic strain 4N24 (Fig. 5A). Importantly, the data revealed that several regulators synergistically cooperated to control expression of the cluster. The regulator NybW controlled expression of *nybQRSTUV*, while the regulators encoding *nybXYZ* modulated transcription of cluster genes further upstream. Therefore, combined elimination of *nybW* plus *nybX* or *nybW* plus *nybXYZ* was needed to override the natural control and release the cluster from repression, whereas single deletion of *nybW*, *nybX*, *nybY*, or *nybZ* was not sufficient. Bacterial gene clusters often contain several cluster-situated regulatory elements (Novakova et al., 2022; Sun et al., 2018; Zhu et al., 2017). The encoded multifunctional regulators can form a complex intricate regulatory network (Tsyplik et al., 2021), as also observed in our study.

Merging all the obtained knowledge, we finally combined the

optimized primary metabolic pathway layout with the optimized layout of the nybomycin biosynthetic pathway. To this end, the deregulated cluster mutants NYB-8 and NYB-9 were equipped with the best targets from primary metabolism. Transformation of NYB-8 and NYB-9 with the integrative plasmid pBT1H-kasOP**-nybF-zwf2* resulted in the new strains NYB-10 (4N24 $\Delta nybWX$ P_{kasOP*} *nybF zwf2*) and NYB-11 (4N24 $\Delta nybWXYZ$ P_{kasOP*} *nybF zwf2*), respectively. Favorably, both cell factories produced more nybomycin than any other strain created (Fig. 6G and H). When tested in batch cultures, NYB-10 accumulated 2510 $\mu\text{g L}^{-1}$ nybomycin, while NYB-11 accumulated 3570 $\mu\text{g L}^{-1}$, more than fourfold more than 4N24 (Fig. 5A). The time to reach the peak titer was approximately 200 h for both strains, compared to 275 h for the basic strain 4N24 (Fig. 3A).

Finally, we benchmarked the strains NYB-8, NYB-9, NYB-10, and NYB-11 on minimal medium with 50 g L⁻¹ mannitol (Fig. 10). All mutants exhibited excellent production performance, with strain NYB-11 performing best during both culture phases and achieving the highest final nybomycin titer of 12 mg L⁻¹. Overall, systems metabolic engineering and a superior bioprocess at high initial substrate levels enabled an almost fifteen-fold increase in production of nybomycin from the original strain. *S. albidoflavus* NYB-11 approached the performance of the best producer known thus far (Kuhl et al., 2021).

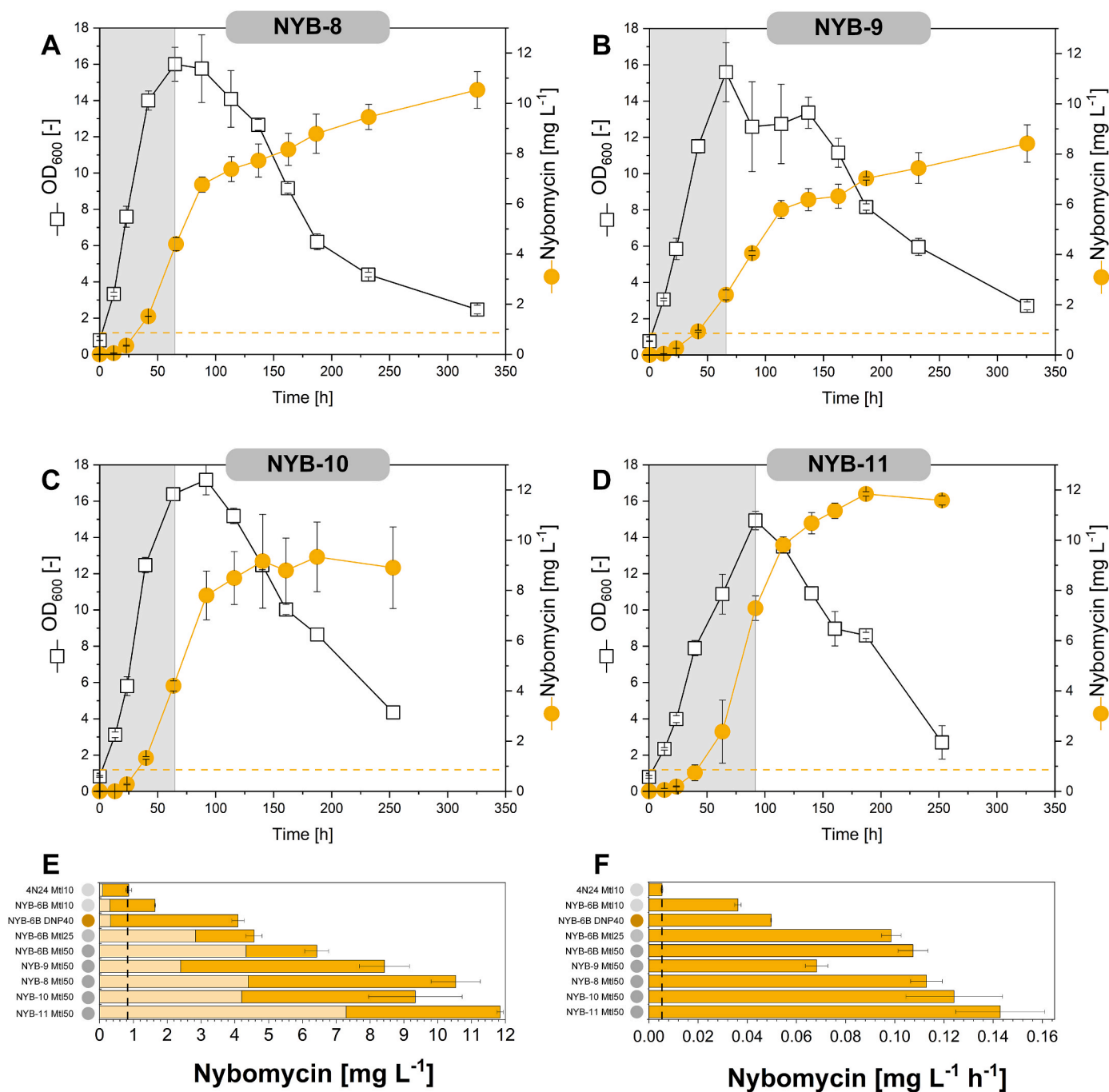


Fig. 10. Benchmarking the created *Streptomyces albidoflavus* nybomycin producers in batch processes. The data show the growth and production profiles of the strains NYB-8 (A), NYB-9 (B), NYB-10 (C), and NYB-11 (D) on minimal medium with 50 g L⁻¹ of mannitol. In addition, the achieved final titre (E) and the maximum volumetric productivity (F) are shown for different mutants (4N24, NYB-6B, NYB-8, NYB-9, NYB-10, and NYB-11). For comparison, the orange dotted line in each plot shows the maximum titer of the basic producer 4N24 (Fig. 3A). The strains were grown on complex medium with 40 g L⁻¹ dextrin (DNP40) and on minimal medium with 10 g L⁻¹ (Mtl10), 25 g L⁻¹ (Mtl25), and 50 g L⁻¹ (Mtl50) of mannitol, respectively. n = 3.

4. Conclusions

As shown, we metabolically engineered *S. albidoflavus* 4N24 (Rodríguez Estevez et al., 2018) into a cell factory to overproduce nybomycin. Several rounds of metabolic engineering provided strains with successively improved nybomycin titers. Notably, deregulation of *nyb* cluster expression through elimination of the regulator gene *nybW* enabled efficient production during the growth phase as well as the stationary phase, substantially shortening the production process. The acceleration appeared useful, as secondary metabolites are produced

mainly in the late growth or stationary phase (Ferraiuolo et al., 2021); thus, industrial processes using *Streptomyces* are usually very long and suffer from low productivities (Pereira et al., 2008).

The chosen host and the established process both supported selective production of nybomycin, which should facilitate purification in the future. All producers of the NYB family created in this work were based on the pre-engineered cluster-free chassis *S. albidoflavus* Del14, eliminating potential interference from native natural products of the host (Myronovskiy et al., 2018). In addition, use of a lean, minimal medium, as shown herein, prevented the typical impurities that result from use of

complex ingredients.

Conceptually, we aimed at systems-wide strain engineering because this approach has proven to be most successful in overproducing amino acids and organic acids, typically demanding a set of different cellular precursors, at very high titers and yields (Becker et al., 2011; Kind et al., 2013, 2014; Rohles et al., 2016). Similarly, synthesis of the nybomycin molecule needed precursors from various routes (Fig. 1B). The best strain, NYB-11, produced 12 mg L⁻¹ nybomycin, fifteenfold more than the basic producer used as a starting point. This improvement was enabled by the combination of targets from primary and secondary metabolism, which synergistically contributed to enhanced production. The achieved performance reached the level of the best producers known thus far and displays an important and encouraging step to explore nybomycin further. However, elevated amounts will be needed for drug optimization through medicinal chemistry, activity and stability testing, toxicity screening, and mode-of-action studies to explore the compound further, requiring more efficient cell factories in the future. To this end, additional rounds of metabolic engineering of *S. albidoflavus* NYB-11 appear to be promising to further improve production efficiency. Additionally, random mutagenesis might be added as a complementary strategy to strain development regarding the largely unexplored nybomycin pathway. In addition, it might be worth testing other genetically accessible *Streptomyces* hosts for heterologous nybomycin production, as engineered strains have different efficiencies in accumulating nybomycin (Myronovskiy et al., 2020).

Beyond nybomycin, it appears straightforward to apply similar systems metabolic engineering approaches to improve other *S. albidoflavus*-based producers created by heterologous cluster expression (Estevez et al., 2020; Myronovskiy et al., 2018). Based on our findings, the synthetic promoter derivatives applied herein can be recommended for broader use, given their constitutive nature, while care should be taken regarding use of *PerME**. While other genetic backgrounds or production media might change the picture observed in this work, we suggest additional case-specific tests with online recording of promoter dynamics.

Credit authorship contribution statement

J.S: Conceptualization, Methodology, Validation, Investigation, Writing - original draft, Writing - review & editing.

M. R. E.: Conceptualization, Methodology, Validation, Investigation, Writing - review & editing.

W. S.: Investigation, Writing - review & editing.

L. G.: Investigation, Writing - review & editing.

M.M. Methodology, Validation, Investigation, Writing - review & editing.

C.R.: Methodology, Validation, Investigation, Writing - review & editing.

J.K.: Funding acquisition, Validation, Formal analysis, Writing - review & editing.

A.L.: Conceptualization, Funding acquisition, Methodology, Validation, Formal analysis, Supervision, Writing - review & editing.

C. W: Conceptualization, Funding acquisition, Methodology, Validation, Formal analysis, Supervision, Writing - original draft, Writing - Writing - review & editing.

Conflicts of interest

There are no conflicts of interest to declare.

Data availability

Data will be made available on request.

Acknowledgments

Christoph Wittmann, Andriy Luzhetskyy, and Jörn Kalinowski acknowledge financial support by the Federal Ministry of Education and Research (BMBF) through the grants Explomare (FK 031B0866) and MyBio (FK 031B0344). Christoph Wittmann further acknowledges funding from the German Research Foundation through grant INST 256/418–1.

Appendix A. Supplementary data

Supplementary data to this article can be found online at <https://doi.org/10.1016/j.ymben.2023.12.004>.

References

- Ahmed, Y., Rebets, Y., Estevez, M.R., Zapp, J., Myronovskiy, M., Luzhetskyy, A., 2020. Engineering of *Streptomyces lividans* for heterologous expression of secondary metabolite gene clusters. *Microb. Cell Factories* 19, 5.
- Aldred, K.J., Kerns, R.J., Osheroff, N., 2014. Mechanism of quinolone action and resistance. *Biochemistry* 53, 1565–1574.
- Arai, M., Kamiya, K., Pruksakorn, P., Sumii, Y., Kotoku, N., Joubert, J.P., Moodley, P., Han, C., Shin, D., Kobayashi, M., 2015. Anti-dormant mycobacterial activity and target analysis of nybomycin produced by a marine-derived *Streptomyces* sp. *Bioorg. Med. Chem.* 23, 3534–3541.
- Bai, C., Zhang, Y., Zhao, X., Hu, Y., Xiang, S., Miao, J., Lou, C., Zhang, L., 2015. Exploiting a precise design of universal synthetic modular regulatory elements to unlock the microbial natural products in *Streptomyces*. *Proc. Natl. Acad. Sci. U. S. A.* 112, 12181–12186.
- Bardell-Cox, O.A., White, A.J.P., Aragon, L., Fuchter, M.J., 2019. Synthetic studies on the reverse antibiotic natural products, the nybomycins. *Medchemcomm* 10, 1438–1444.
- Barton, N., Horbal, L., Starck, S., Kohlstedt, M., Luzhetskyy, A., Wittmann, C., 2018. Enabling the valorization of guaiacol-based lignin: integrated chemical and biochemical production of cis,cis-muconic acid using metabolically engineered *Amycolatopsis* sp. ATCC 39116. *Metab. Eng.* 45, 200–210.
- Becker, J., Klopprogge, C., Herold, A., Zelder, O., Bolten, C.J., Wittmann, C., 2007. Metabolic flux engineering of L-lysine production in *Corynebacterium glutamicum*—over expression and modification of G6P dehydrogenase. *J. Biotechnol.* 132, 99–109.
- Becker, J., Klopprogge, C., Wittmann, C., 2008. Metabolic responses to pyruvate kinase deletion in lysine producing *Corynebacterium glutamicum*. *Microb. Cell Factories* 7, 8.
- Becker, J., Kuhl, M., Kohlstedt, M., Starck, S., Wittmann, C., 2018. Metabolic engineering of *Corynebacterium glutamicum* for the production of cis, cis-muconic acid from lignin. *Microb. Cell Factories* 17, 115.
- Becker, J., Zelder, O., Haefner, S., Schröder, H., Wittmann, C., 2011. From zero to hero—Design-based systems metabolic engineering of *Corynebacterium glutamicum* for L-lysine production. *Metab. Eng.* 13, 159–168.
- Bednarsz, B., Kotowska, M., Pawlik, K.J., 2019. Multi-level regulation of coelimycin synthesis in *Streptomyces coelicolor* A3(2). *Appl. Microbiol. Biotechnol.* 103, 6423–6434.
- Beganovic, S., Rückert-Reed, C., Sucipto, H., Shu, W., Glaser, L., Patschkowski, T., Struck, B., Kalinowski, J., Luzhetskyy, A., Wittmann, C., 2023. Systems biology of industrial oxytetracycline production in *Streptomyces rimosus*: the secrets of a mutagenized hyperproducer. *Microb. Cell Factories* 22, 222.
- Bibb, M.J., White, J., Ward, J.M., Janssen, G.R., 1994. The mRNA for the 23S rRNA methylase encoded by the ermE gene of *Saccharopolyspora erythraea* is translated in the absence of a conventional ribosome-binding site. *Mol. Microbiol.* 14, 533–545.
- Blower, T.R., Williamson, B.H., Kerns, R.J., Berger, J.M., 2016. Crystal structure and stability of gyrase–fluoroquinolone cleaved complexes from *Mycobacterium tuberculosis*. *Proc. Natl. Acad. Sci. U. S. A.* 113, 1706–1713.
- Bobek, J., Mikulová, A., Setinová, D., Elliot, M., Čihák, M., 2021. 6S-Like scr3559 RNA affects development and antibiotic production in *Streptomyces coelicolor*. *Microorganisms* 9.
- Chen, D., Zhang, Q., Cen, P., Xu, Z., Liu, W., 2012. Improvement of FK506 production in *Streptomyces tsukubaensis* by genetic enhancement of the supply of unusual polyketide extender units via utilization of two distinct site-specific recombination systems. *Appl. Environ. Microbiol.* 78, 5093–5103.
- Christmann, J., Cao, P., Becker, J., Desiderato, C.K., Goldbeck, O., Riedel, C.U., Kohlstedt, M., Wittmann, C., 2023. High-efficiency production of the antimicrobial peptide pediocin PA-1 in metabolically engineered *Corynebacterium glutamicum* using a microaerobic process at acidic pH and elevated levels of bivalent calcium ions. *Microb. Cell Factories* 22, 41.
- Dalla Pozza, E., Dando, I., Pacchiana, R., Liboi, E., Scupoli, M.T., Donadelli, M., Palmieri, M., 2020. Regulation of succinate dehydrogenase and role of succinate in cancer. *Semin. Cell Dev. Biol.* 98, 4–14.
- Deguchi, T., Fukuoka, A., Yasuda, M., Nakano, M., Ozeki, S., Kanematsu, E., Nishino, Y., Ishihara, S., Ban, Y., Kawada, Y., 1997. Alterations in the GyrA subunit of DNA gyrase and the ParC subunit of topoisomerase IV in quinolone-resistant clinical isolates of *Klebsiella pneumoniae*. *Antimicrob. Agents Chemother.* 41, 699–701.
- Drlica, K., Hiasa, H., Kerns, R., Malik, M., Mustaev, A., Zhao, X., 2009. Quinolones: action and resistance updated. *Curr. Top. Med. Chem.* 9, 981–998.

- Egawa, K., Yamori, T., Nosaka, C., Kunimoto, S., Takeuchi, T., Nos, K., 2000. Deoxynybomycin is a selective anti-tumor agent inducing apoptosis and inhibiting topoisomerase I. *Biol. Pharm. Bull.* 23, 1036–1040.
- Estevez, M.R., Gummerlich, N., Myronovskiy, M., Zapp, J., Luzhetskyy, A., 2020. Benzantronic acid, a novel metabolite from *Streptomyces albus* Del14 expressing the nybomycin gene cluster. *Front. Chem.* 7.
- Eudes, A., Juminaga, D., Baidoo, E.E., Collins, F.W., Keasling, J.D., Loque, D., 2013. Production of hydroxycinnamoyl anthranilates from glucose in *Escherichia coli*. *Microb. Cell Factories* 12, 62.
- Euverink, G.-J., 1995. Aromatic Amino Acid Biosynthesis in Actinomycetes.
- Ferraiuolo, S.B., Cammarota, M., Schiraldi, C., Restaino, O.F., 2021. Streptomyces as platform for biotechnological production processes of drugs. *Appl. Microbiol. Biotechnol.* 105, 551–568.
- Forbis, R.M., Rinehart Jr., K.L., 1970. Nybomycin. IV. Total synthesis of deoxynybomycin. *J. Am. Chem. Soc.* 92, 6995–6996.
- Forbis, R.M., Rinehart Jr., K.L., 1971. Nybomycin. V. Total synthesis of nybomycin. *J. Antibiot. (Tokyo)* 24, 326–327.
- Forbis, R.M., Rinehart Jr., K.L., 1973. Nybomycin. VII. Preparative routes to nybomycin and deoxynybomycin. *J. Am. Chem. Soc.* 95, 5003–5013.
- Fujita, Y., Matsuoka, H., Hirooka, K., 2007. Regulation of fatty acid metabolism in bacteria. *Mol. Microbiol.* 66, 829–839.
- García-Gutiérrez, C., Aparicio, T., Torres-Sánchez, L., Martínez-García, E., de Lorenzo, V., Villar, C.J., Lombo, F., 2020. Multifunctional SEVA shuttle vectors for actinomycetes and Gram-negative bacteria. *Microbiol.* 9, 1135–1149.
- Giesselmann, G., Dietrich, D., Jungmann, L., Kohlstedt, M., Jeon, E.J., Yim, S.S., Sommer, F., Zimmer, D., Muhlhaus, T., Schroda, M., Jeong, K.J., Becker, J., Wittmann, C., 2019. Metabolic engineering of *Corynebacterium glutamicum* for high-level ectoine production: design, combinatorial assembly, and implementation of a transcriptionally balanced heterologous ectoine pathway. *Biotechnol. J.* 14, e1800417.
- Gläser, L., Kuhl, M., Stegmüller, J., Ruckert, C., Myronovskiy, M., Kalinowski, J., Luzhetskyy, A., Wittmann, C., 2021a. Superior production of heavy pamamycin derivatives using a bkdR deletion mutant of *Streptomyces albus* J1074/R2. *Microb. Cell Factories* 20, 111.
- Gläser, L., Kuhl, M., Stegmüller, J., Ruckert, C., Myronovskiy, M., Kalinowski, J., Luzhetskyy, A., Wittmann, C., 2021b. Superior production of heavy pamamycin derivatives using a bkdR deletion mutant of *Streptomyces albus* J1074/R2. *Microb. Cell Factories* 20, 111.
- Gramajo, H.C., Takano, E., Bibb, M.J., 1993. Stationary-phase production of the antibiotic actinorhodin in *Streptomyces coelicolor* A3(2) is transcriptionally regulated. *Mol. Microbiol.* 7, 837–845.
- Gregory, M.A., Till, R., Smith, M.C., 2003. Integration site for *Streptomyces* phage phiBT1 and development of site-specific integrating vectors. *J. Bacteriol.* 185, 5320–5323.
- Hergenrother, P.J., Leys, D., 2018. Topoisomerase inhibitors with antibacterial and anticancer properties. US Patent 11274106.
- Hilker, R., Stadermann, K.B., Doppmeier, D., Kalinowski, J., Stoye, J., Straube, J., Winnebold, J., Goesmann, A., 2014. ReadXplorer—visualization and analysis of mapped sequences. *Bioinformatics* 30, 2247–2254.
- Hiramatsu, K., Igarashi, M., Morimoto, Y., Baba, T., Umekita, M., Akamatsu, Y., 2012. Curing bacteria of antibiotic resistance: reverse antibiotics, a novel class of antibiotics in nature. *Int. J. Antimicrob. Agents* 39, 478–485.
- Hiramatsu, K., Sasaki, T., Morimoto, Y., 2015. Future chemotherapy preventing emergence of multi-antibiotic resistance. *Juntendo Medical Journal* 61, 249–256.
- Hoffmann, S.L., Jungmann, L., Schiefelbein, S., Peyriga, L., Cahoreau, E., Portais, J.C., Becker, J., Wittmann, C., 2018. Lysine production from the sugar alcohol mannitol: design of the cell factory *Corynebacterium glutamicum* SEA-3 through integrated analysis and engineering of metabolic pathway fluxes. *Metab. Eng.* 47, 475–487.
- Hoffmann, S.L., Kohlstedt, M., Jungmann, L., Hutter, M., Poblete-Castro, I., Becker, J., Wittmann, C., 2021. Cascaded valorization of brown seaweed to produce l-lysine and value-added products using *Corynebacterium glutamicum* streamlined by systems metabolic engineering. *Metab. Eng.* 67, 293–307.
- Holt, T.G., Chang, C., Laurent-Winter, C., Murakami, T., Garrels, J.I., Davies, J.E., Thompson, C.J., 1992. Global changes in gene expression related to antibiotic synthesis in *Streptomyces hygroscopicus*. *Mol. Microbiol.* 6, 969–980.
- Huang, D., Li, S., Xia, M., Wen, J., Jia, X., 2013. Genome-scale metabolic network guided engineering of *Streptomyces tsukubaensis* for FK506 production improvement. *Microb. Cell Factories* 12, 52.
- Huang, S., Millar, A.H., 2013. Succinate dehydrogenase: the complex roles of a simple enzyme. *Curr. Opin. Plant Biol.* 16, 344–349.
- Huo, L., Rachid, S., Stadler, M., Wenzel, S.C., Müller, R., 2012. Synthetic biotechnology to study and engineer ribosomal bottomycin biosynthesis. *Chem. Biol.* 19, 1278–1287.
- Hwang, M.-S., Rohlena, J., Dong, L.-F., Neuzil, J., Grimm, S., 2014. Powerhouse down: complex II dissociation in the respiratory chain. *Mitochondrion* 19, 20–28.
- Hwang, S., Lee, N., Jeong, Y., Lee, Y., Kim, W., Cho, S., Palsson, B.O., Cho, B.K., 2019. Primary transcriptome and translome analysis determines transcriptional and translational regulatory elements encoded in the *Streptomyces clavuligerus* genome. *Nucleic Acids Res.* 47, 6114–6129.
- Ian, E., Malko, D.B., Sekurova, O.N., Bredholt, H., Ruckert, C., Borisova, M.E., Albersmeier, A., Kalinowski, J., Gelfand, M.S., Zotchev, S.B., 2014. Genomics of sponge-associated *Streptomyces* spp. closely related to *Streptomyces albus* J1074: insights into marine adaptation and secondary metabolite biosynthesis potential. *PLoS One* 9, e96719.
- Ikedo, M., 2006. Towards bacterial strains overproducing L-tryptophan and other aromatics by metabolic engineering. *Appl. Microbiol. Biotechnol.* 69, 615–626.
- Jin, X.M., Chang, Y.K., Lee, J.H., Hong, S.K., 2017. Effects of increased NADPH concentration by metabolic engineering of the pentose phosphate pathway on antibiotic production and sporulation in streptomycetes lividans TK24. *J. Microbiol. Biotechnol.* 27, 1867–1876.
- Jin, Z., Jin, X., Jin, Q., 2010. Conjugal transferring of resistance gene ptr for improvement of pristinamycin-producing *Streptomyces pristinaespiralis*. *Appl. Biochem. Biotechnol.* 160, 1853–1864.
- Jones, J.A., Vernacchio, V.R., Lachance, D.M., Lebovich, M., Fu, L., Shirke, A.N., Schultz, V.L., Cress, B., Linhardt, R.J., Koffas, M.A., 2015. ePathOptimize: a combinatorial approach for transcriptional balancing of metabolic pathways. *Sci. Rep.* 5, 11301.
- Jovanovic Gasovic, S., Dietrich, D., Gläser, L., Cao, P., Kohlstedt, M., Wittmann, C., 2023. Multi-omics view of recombinant *Yarrowia lipolytica*: enhanced ketogenic amino acid catabolism increases polyketide-synthase-driven docosahexaenoic production to high selectivity at the gram scale. *Metab. Eng.* 80, 45–65.
- Kaiser, J.C., Heinrichs, D.E., 2018. Branching out: alterations in bacterial physiology and virulence due to branched-chain amino acid deprivation. *mBio* 9.
- Kallifidas, D., Jiang, G., Ding, Y., Luesch, H., 2018. Rational engineering of *Streptomyces albus* J1074 for the overexpression of secondary metabolite gene clusters. *Microb. Cell Factories* 17, 25.
- Kieser, T., Bibb, M.J., Buttner, M.J., Chater, K.F., Hopwood, D.A., 2000. *Practical Streptomyces Genetics*. The John Innes Foundation, Norwich, UK.
- Kikuchi, Y., Tsujimoto, K., Kurahashi, O., 1997. Mutational analysis of the feedback sites of phenylalanine-sensitive 3-deoxy-D-arabino-heptulosonate-7-phosphate synthase of *Escherichia coli*. *Appl. Environ. Microbiol.* 63, 761–762.
- Kind, S., Becker, J., Wittmann, C., 2013. Increased lysine production by flux coupling of the tricarboxylic acid cycle and the lysine biosynthetic pathway—metabolic engineering of the availability of succinyl-CoA in *Corynebacterium glutamicum*. *Metab. Eng.* 15, 184–195.
- Kind, S., Neubauer, S., Becker, J., Yamamoto, M., Völkert, M., Abendroth, G.V., Zelder, O., Wittmann, C., 2014. From zero to hero - production of bio-based nylon from renewable resources using engineered *Corynebacterium glutamicum*. *Metab. Eng.* 25, 113–123.
- Kohlstedt, M., Sappa, P.K., Meyer, H., Maass, S., Zapras, A., Hoffmann, T., Becker, J., Steil, L., Hecker, M., van Dijk, J.M., Lalk, M., Mader, U., Stülke, J., Bremer, E., Völker, U., Wittmann, C., 2014. Adaptation of *Bacillus subtilis* carbon core metabolism to simultaneous nutrient limitation and osmotic challenge: a multi-omics perspective. *Environ. Microbiol.* 16, 1898–1917.
- Kohlstedt, M., Starck, S., Barton, N., Stolzenberger, J., Selzer, M., Mehlmann, K., Schneider, R., Pleissner, D., Rinkel, J., Dickschat, J.S., Venus, J., van Duuren, J.B.J. H., Wittmann, C., 2018. From lignin to nylon: cascaded chemical and biochemical conversion using metabolically engineered *Pseudomonas putida*. *Metab. Eng.* 47, 279–293.
- Kohlstedt, M., Weimer, A., Weiland, F., Stolzenberger, J., Selzer, M., Sanz, M., Kramps, L., Wittmann, C., 2022. Biobased PET from lignin using an engineered cis-cis-muconate-producing *Pseudomonas putida* strain with superior robustness, energy and redox properties. *Metab. Eng.* 72, 337–352.
- Komaki, H., Hosoyama, A., Kimura, A., Ichikawa, N., Igarashi, Y., Tamura, T., 2020. Classification of *Streptomyces hyalinalis* Hamada and Yokoyama as *Embleya hyalinalis* sp. nov., the second species in the genus *Embleya*, and emendation of the genus *Embleya*. *Int. J. Syst. Evol. Microbiol.* 70, 1591–1595.
- Kormanec, J., Novakova, R., Mingyar, E., Feckova, L., 2014. Intriguing properties of the angucycline antibiotic auricin and complex regulation of its biosynthesis. *Appl. Microbiol. Biotechnol.* 98, 45–60.
- Kuhl, M., Gläser, L., Rebets, Y., Ruckert, C., Sarkar, N., Hartsch, T., Kalinowski, J., Luzhetskyy, A., Wittmann, C., 2020. Microparticles globally reprogram *Streptomyces albus* toward accelerated morphogenesis, streamlined carbon core metabolism, and enhanced production of the antituberculosis polyketide pamamycin. *Biotechnol. Bioeng.* 117, 3858–3875.
- Kuhl, M., Ruckert, C., Glaser, L., Beganovic, S., Luzhetskyy, A., Kalinowski, J., Wittmann, C., 2021. Microparticles enhance the formation of seven major classes of natural products in native and metabolically engineered actinobacteria through accelerated morphological development. *Biotechnol. Bioeng.* 118, 3076–3093.
- Labes, G., Bibb, M., Wohlleben, W., 1997. Isolation and characterization of a strong promoter element from the *Streptomyces ghanensis* phage P19 using the gentamicin resistance gene (aacC1) of Tn 1696 as reporter. *Microbiology* 143 (Pt 5), 1503–1512.
- Langmead, B., Salzberg, S.L., 2012. Fast gapped-read alignment with Bowtie 2. *Nat. Methods* 9, 357.
- Lee, Y., Lee, N., Hwang, S., Kim, W., Cho, S., Palsson, B.O., Cho, B.K., 2022. Genome-scale analysis of genetic regulatory elements in *Streptomyces avermitilis* MA-4680 using transcript boundary information. *BMC Genom.* 23, 68.
- Liao, H.F., Lin, L.L., Chien, H.R., Hsu, W.H., 2001. Serine 187 is a crucial residue for allosteric regulation of *Corynebacterium glutamicum* 3-deoxy-D-arabino-heptulosonate-7-phosphate synthase. *FEMS Microbiol. Lett.* 194, 59–64.
- Liu, G., Chater, K.F., Chandra, G., Niu, G., Tan, H., 2013. Molecular regulation of antibiotic biosynthesis in streptomycetes. *Microbiol. Mol. Biol. Rev.* 77, 112–143.
- Love, M.I., Huber, W., Anders, S., 2014. Moderated estimation of fold change and dispersion for RNA-seq data with DESeq2. *Genome Biol.* 15, 550.
- Lu, C., Zhang, X., Jiang, M., Bai, L., 2016. Enhanced salinomycin production by adjusting the supply of polyketide extender units in *Streptomyces albus*. *Metab. Eng.* 35, 129–137.
- Ma, Z., Hu, Y., Liao, Z., Xu, J., Xu, X., Bechthold, A., Yu, X., 2020. Cloning and overexpression of the toy cluster for titer improvement of toyocamycin in *Streptomyces diastatochromogenes*. *Front. Microbiol.* 11, 2074.

- Mao, X.M., Luo, S., Li, Y.Q., 2017. Negative regulation of daptomycin production by DepR2, an ArsR-family transcriptional factor. *J. Ind. Microbiol. Biotechnol.* 44, 1653–1658.
- Massey, L.K., Sokatch, J.R., Conrad, R.S., 1976. Branched-chain amino acid catabolism in bacteria. *Bacteriol. Rev.* 40, 42–54.
- Meza, E., Becker, J., Bolivar, F., Gosset, G., Wittmann, C., 2012. Consequences of phosphoenolpyruvate:sugar phosphotransferase system and pyruvate kinase isozymes inactivation in central carbon metabolism flux distribution in *Escherichia coli*. *Microb. Cell Factories* 11, 127.
- Mo, J., Wang, S., Zhang, W., Li, C., Deng, Z., Zhang, L., Qu, X., 2019. Efficient editing DNA regions with high sequence identity in actinomycetal genomes by a CRISPR-Cas9 system. *Synthetic and systems biotechnology* 4, 86–91.
- Morimoto, Y., Baba, T., Sasaki, T., Hiramatsu, K., 2015. Apigenin as an anti-quinolone-resistance antibiotic. *Int. J. Antimicrob. Agents* 46, 666–673.
- Myronovskiy, M., Luzhetskyy, A., 2016. Native and engineered promoters in natural product discovery. *Nat. Prod. Rep.* 33, 1006–1019.
- Myronovskiy, M., Rosenkranz, B., Nadmid, S., Pujic, P., Normand, P., Luzhetskyy, A., 2018. Generation of a cluster-free *Streptomyces albus* chassis strains for improved heterologous expression of secondary metabolite clusters. *Metab. Eng.* 49, 316–324.
- Myronovskiy, M., Rosenkranz, B., Stierhof, M., Petzke, L., Seiser, T., Luzhetskyy, A., 2020. Identification and heterologous expression of the albuscin gene cluster from the marine strain *Streptomyces albus* subsp. *chlorinus* NRRL B-24108. *Microorganisms* 8.
- Novakova, R., Mingyar, E., Feckova, L., Homerova, D., Csolleiova, D., Rezuchova, B., Sevcikova, B., Javorova, R., Kormanec, J., 2022. A new family of transcriptional regulators activating biosynthetic gene clusters for secondary metabolites. *Int. J. Mol. Sci.* 23.
- Nussbaum, F., Ebbinghaus, A., Mayer-Bartschmid, A., Zitzmann, W., Wiese, W.B., Stadler, M., Anlauf, S., 2009. CDC25 Inhibitors. EP Patent 2,130,831.
- Park, S.J., Tseng, C.P., Gunsalus, R.P., 1995. Regulation of succinate dehydrogenase (sdhCDAB) operon expression in *Escherichia coli* in response to carbon supply and anaerobiosis: role of ArcA and Fnr. *Mol. Microbiol.* 15, 473–482.
- Parkinson, E.I., Bair, J.S., Nakamura, B.A., Lee, H.Y., Kuttab, H.I., Southgate, E.H., Lezmi, S., Lau, G.W., Hergenrother, P.J., 2015a. Deoxybomycins inhibit mutant DNA gyrase and rescue mice infected with fluoroquinolone-resistant bacteria. *Nat. Commun.* 6, 6947.
- Parkinson, E.I., Bair, J.S., Nakamura, B.A., Lee, H.Y., Kuttab, H.I., Southgate, E.H., Lezmi, S., Lau, G.W., Hergenrother, P.J., 2015b. Deoxybomycins inhibit mutant DNA gyrase and rescue mice infected with fluoroquinolone-resistant bacteria. *Nat. Commun.* 6, 6947.
- Parthasarathy, A., Cross, P.J., Dobson, R.C.J., Adams, L.E., Savka, M.A., Hudson, A.O., 2018. A three-ring circus: metabolism of the three proteogenic aromatic amino acids and their role in the health of plants and animals. *Front. Mol. Biosci.* 5, 29.
- Pauli, S., Kohlstedt, M., Lamber, J., Weiland, F., Becker, J., Wittmann, C., 2023. Systems metabolic engineering upgrades *Corynebacterium glutamicum* for selective high-level production of the chiral drug precursor and cell-protective extremolyte L-pipecolic acid. *Metab. Eng.* 77, 100–117.
- Paulus, C., Myronovskiy, M., Zapp, J., Rodriguez Estevez, M., Lopatniuk, M., Rosenkranz, B., Paluszczak, A., Luzhetskyy, A., 2022. Miramides A-D: identification of detoxin-like depsipeptides after heterologous expression of a hybrid NRPS-PKS gene cluster from *Streptomyces mirabilis* Lu17588. *Microorganisms* 10.
- Pavoncello, V., Barras, F., Bouveret, E., 2022. Degradation of exogenous fatty acids in *Escherichia coli*. *Biomolecules* 12.
- Pereira, T., Nikodinovic, J., Nakazono, C., Dennis, G.R., Barrow, K.D., Chuck, J.A., 2008. Community structure and antibiotic production of *Streptomyces nodosus* bioreactors cultured in liquid environments. *Microb. Biotechnol.* 1, 373–381.
- Peters-Wendisch, P.G., Eikmanns, B.J., Thierbach, G., Bachmann, B., Sahl, H., 1993. Phosphoenolpyruvate carboxylase in *Corynebacterium glutamicum* is dispensable for growth and lysine production. *FEMS Microbiol. Lett.* 112, 269–274.
- Pizer, E.S., Thupari, J., Han, W.F., Pinn, M.L., Chrest, F.J., Frehywot, G.L., Townsend, C.A., Kuhajda, F.P., 2000. Malonyl-coenzyme-A is a potential mediator of cytotoxicity induced by fatty-acid synthase inhibition in human breast cancer cells and xenografts. *Cancer Res.* 60, 213–218.
- Price, L.B., Vogler, A., Pearson, T., Busch, J.D., Schupp, J.M., Keim, P., 2003. In vitro selection and characterization of *Bacillus anthracis* mutants with high-level resistance to ciprofloxacin. *Antimicrob. Agents Chemother.* 47, 2362–2365.
- Qiu, J., Zhuo, Y., Zhu, D., Zhou, X., Zhang, L., Bai, L., Deng, Z., 2011. Overexpression of the ABC transporter AvtAB increases avermectin production in *Streptomyces avermitilis*. *Appl. Microbiol. Biotechnol.* 92, 337–345.
- Richter, M.F., Drown, B.S., Riley, A.P., Garcia, A., Shirai, T., Svec, R.L., Hergenrother, P. J., 2017. Predictive compound accumulation rules yield a broad-spectrum antibiotic. *Nature* 545, 299–304.
- Rodrigues, A.L., Trachtman, N., Becker, J., Lohanatha, A.F., Blotenberg, J., Bolten, C.J., Korneli, C., de Souza Lima, A.O., Porto, L.M., Sprenger, G.A., Wittmann, C., 2013. Systems metabolic engineering of *Escherichia coli* for production of the antitumor drugs violacein and deoxyviolacein. *Metab. Eng.* 20, 29–41.
- Rodriguez, A., Martinez, J.A., Flores, N., Escalante, A., Gosset, G., Bolivar, F., 2014. Engineering *Escherichia coli* to overproduce aromatic amino acids and derived compounds. *Microb. Cell Factories* 13, 126.
- Rodriguez Estevez, M., Myronovskiy, M., Gummerlich, N., Nadmid, S., Luzhetskyy, A., 2018. Heterologous expression of the nybomycin gene cluster from the marine strain *Streptomyces albus* subsp. *chlorinus* NRRL B-24108. *Mar. Drugs* 16.
- Rohles, C., Pauli, S., Giesselmann, G., Kohlstedt, M., Becker, J., Wittmann, C., 2022. Systems metabolic engineering of *Corynebacterium glutamicum* eliminates all by-products for selective and high-yield production of the platform chemical 5-aminovaleate. *Metab. Eng.* 73, 168–181.
- Rohles, C.M., Giesselmann, G., Kohlstedt, M., Wittmann, C., Becker, J., 2016. Systems metabolic engineering of *Corynebacterium glutamicum* for the production of the carbon-5 platform chemicals 5-aminovaleate and glutarate. *Microb. Cell Factories* 15, 154.
- Rohles, C.M., Gläser, L., Kohlstedt, M., Gießelmann, G., Pearson, S., del Campo, A., Becker, J., Wittmann, C., 2018. A bio-based route to the carbon-5 chemical glutaric acid and to bionylon-6,5 using metabolically engineered *Corynebacterium glutamicum*. *Green Chem.* 20, 4662–4674.
- Ruiz, B., Chavez, A., Forero, A., Garcia-Huante, Y., Romero, A., Sanchez, M., Rocha, D., Sanchez, B., Rodriguez-Sanoja, R., Sanchez, S., Langley, E., 2010. Production of microbial secondary metabolites: regulation by the carbon source. *Crit. Rev. Microbiol.* 36, 146–167.
- Sambrook, J.F., Russell, D.W., 2001. *Molecular Cloning: A Laboratory Manual*, third ed. Cold Spring Harbor Laboratory Press. 1,2 and 3.
- Sander, T., Farke, N., Diehl, C., Kuntz, M., Glatzer, T., Link, H., 2019. Allosteric feedback inhibition enables robust amino acid biosynthesis in *E. coli* by enforcing enzyme overabundance. *Cell Syst* 8, 66–75 e8.
- Schilling, O., Frick, O., Herzberg, C., Ehrenreich, A., Heinzl, E., Wittmann, C., Stülke, J., 2007. Transcriptional and metabolic responses of *Bacillus subtilis* to the availability of organic acids: transcription regulation is important but not sufficient to account for metabolic adaptation. *Appl. Environ. Microbiol.* 73, 499–507.
- Schwechheimer, S.K., Becker, J., Peyriga, L., Portais, J.C., Sauer, D., Müller, R., Hoff, B., Haefner, S., Schroder, H., Zelder, O., Wittmann, C., 2018a. Improved riboflavin production with *Ashbya gossypii* from vegetable oil based on (13)C metabolic network analysis with combined labeling analysis by GC/MS, LC/MS, 1D, and 2D NMR. *Metab. Eng.* 47, 357–373.
- Schwechheimer, S.K., Becker, J., Peyriga, L., Portais, J.C., Wittmann, C., 2018b. Metabolic flux analysis in *Ashbya gossypii* using (13)C-labeled yeast extract: industrial riboflavin production under complex nutrient conditions. *Microb. Cell Factories* 17, 162.
- Schwentner, A., Feith, A., Munch, E., Stiefelmaier, J., Lauer, I., Favilli, L., Massner, C., Ohrlin, J., Grund, B., Huser, A., Takors, R., Blombach, B., 2019. Modular systems metabolic engineering enables balancing of relevant pathways for l-histidine production with *Corynebacterium glutamicum*. *Biotechnol. Biofuels* 12, 65.
- Seghezzi, N., Amar, P., Koebmann, B., Jensen, P.R., Virolle, M.J., 2011. The construction of a library of synthetic promoters revealed some specific features of strong *Streptomyces* promoters. *Appl. Microbiol. Biotechnol.* 90, 615–623.
- Seyedsayamdost, M.R., 2019. Toward a global picture of bacterial secondary metabolism. *J. Ind. Microbiol. Biotechnol.* 46, 301–311.
- Siegl, T., Tokovenko, B., Myronovskiy, M., Luzhetskyy, A., 2013. Design, construction and characterisation of a synthetic promoter library for fine-tuned gene expression in actinomycetes. *Metab. Eng.* 19, 98–106.
- Strelitz, F., Flon, H., Asheshov, I.N., 1955. Nybomycin, a new antibiotic with antiphage and antibacterial properties. *Proc. Natl. Acad. Sci. U. S. A.* 41, 620–624.
- Sun, L., Zeng, J., Cui, P., Wang, W., Yu, D., Zhan, J., 2018. Manipulation of two regulatory genes for efficient production of chromomycins in *Streptomyces reisei*. *Biotechnol. Bioeng.* 12, 9.
- Team, R.C., 2014. R: A Language and Environment for Statistical Computing. R Foundation for Statistical Computing, Vienna, Austria.
- Tippmann, S., Ferreira, R., Siewers, V., Nielsen, J., Chen, Y., 2017. Effects of acetoacetyl-CoA synthase expression on production of farnesene in *Saccharomyces cerevisiae*. *J. Ind. Microbiol. Biotechnol.* 44, 911–922.
- Tsyplik, O., Makitrynskyi, R., Yan, X., Koch, H.G., Paululat, T., Bechthold, A., 2021. Regulatory control of rishirilide(s) biosynthesis in *Streptomyces bottropensis*. *Microorganisms* 9.
- van Wezel, G.P., van der Meulen, J., Kawamoto, S., Luiten, R.G., Koerten, H.K., Kraal, B., 2000. ssgA is essential for sporulation of *Streptomyces coelicolor* A3(2) and affects hyphal development by stimulating septum formation. *J. Bacteriol.* 182, 5653–5662.
- Vila, J., Ruiz, J., Goni, P., Marcos, A., Jimenez de Anta, T., 1995. Mutation in the *gyrA* gene of quinolone-resistant clinical isolates of *Acinetobacter baumannii*. *Antimicrob. Agents Chemother.* 39, 1201–1203.
- Vila, J., Ruiz, J., Marco, F., Barcelo, A., Goni, P., Giral, E., Jimenez de Anta, T., 1994. Association between double mutation in *gyrA* gene of ciprofloxacin-resistant clinical isolates of *Escherichia coli* and MICs. *Antimicrob. Agents Chemother.* 38, 2477–2479.
- Walker, G.E., Dunbar, B., Hunter, I.S., Nimmo, H.G., Coggins, J.R., 1996. Evidence for a novel class of microbial 3-deoxy-D-arabino-heptulosonate-7-phosphate synthase in *Streptomyces coelicolor* A3(2), *Streptomyces rimosus* and *Neurospora crassa*. *Microbiology* 142 (Pt 8), 1973–1982.
- Wang, X., Elshahawi, S.I., Ponomareva, L.V., Ye, Q., Liu, Y., Copley, G.C., Hower, J.C., Hatcher, B.E., Kharel, M.K., Van Lanen, S.G., She, Q.B., Voss, S.R., Thorson, J.S., Shaaban, K.A., 2019. Structure determination, functional characterization, and biosynthetic implications of nybomycin metabolites from a mining reclamation site-associated streptomyces. *J. Nat. Prod.* 82, 3469–3476.
- Warnes, M.G.R., Bolker, B., Bonebakker, L., Gentleman, R., 2016. Package ‘gplots’. Various R Programming Tools for Plotting Data.
- Weiland, F., Barton, N., Kohlstedt, M., Becker, J., Wittmann, C., 2023. Systems metabolic engineering upgrades *Corynebacterium glutamicum* to high-efficiency *cis*, *cis*-muonic acid production from lignin-based aromatics. *Metab. Eng.* 75, 153–169.
- Werner, G., Fleige, C., Ewert, B., Laverde-Gomez, J.A., Klare, I., Witte, W., 2010. High-level ciprofloxacin resistance among hospital-adapted *Enterococcus faecium* (CC17). *Int. J. Antimicrob. Agents* 35, 119–125.
- Yao, Y.F., Wang, C.S., Qiao, J., Zhao, G.R., 2013. Metabolic engineering of *Escherichia coli* for production of salvanic acid A via an artificial biosynthetic pathway. *Metab. Eng.* 19, 79–87.
- Yin, S., Wang, X., Shi, M., Yuan, F., Wang, H., Jia, X., Sun, J., Liu, T., Yang, K., Zhang, Y., Fan, K., Li, Z., 2017. Improvement of oxytetracycline production mediated via

- cooperation of resistance genes in *Streptomyces rimosus*. *Sci. China Life Sci.* 60, 992–999.
- Zakalyukina, Y.V., Birykov, M.V., Lukianov, D.A., Shiriaev, D.I., Komarova, E.S., Skvortsov, D.A., Kostyukevich, Y., Tashlitsky, V.N., Polshakov, V.I., Nikolaev, E., Sergiev, P.V., Osterman, I.A., 2019. Nybomycin-producing *Streptomyces* isolated from carpenter ant *Camponotus vagus*. *Biochimie* 160, 93–99.
- Zhang, H., Stephanopoulos, G., 2013. Engineering *E. coli* for caffeic acid biosynthesis from renewable sugars. *Appl. Microbiol. Biotechnol.* 97, 3333–3341.
- Zhu, M., Zhang, F., Gan, T., Lin, J., Duan, Y., Zhu, X., 2022. Deciphering the pathway-specific regulatory network for production of ten-membered enediynes Tiancimycins in *Streptomyces* sp. CB03234-S. *Microb. Cell Factories* 21, 188.
- Zhu, Z., Li, H., Yu, P., Guo, Y., Luo, S., Chen, Z., Mao, X., Guan, W., Li, Y., 2017. SlnR is a positive pathway-specific regulator for salinomycin biosynthesis in *Streptomyces albus*. *Appl. Microbiol. Biotechnol.* 101, 1547–1557.